NASA CR-177,022

A Reproduced Copy

OF

NASA CR-177,022

JIAA TR - 74

ANALYTICAL OBSERVATIONS ON THE AERODYNAMICS OF A DELTA WING WITH LEADING EDGE FLAPS

BY

Sejong Oh and Domingo Tavella

Stanford University
Department of Aeronautics and Astronautics
Stanford, CA 94305

MARCH 86

ABSTRACT

The effect of a leading edge flap on the aerodynamics of a low aspect ratio delta wing is studied analytically. The separated flow field about the wing is represented by a simple vortex model composed of a conical straight vortex sheet and a concentrated vortex. The analysis is carried out in the cross-flow plane by mapping the wing trace, by means of the Schwarz-Christoffel transformation into the real axis of the transformed plane. Particular attention is given to the influence of angle of attack and flap deflection angle on lift and drag forces. Both lift and drag decrease with flap deflection, while the lift-to-drag ratio increases. A simple coordinate transformation is used to obtain a closed form expression for the lift-to-drag ratio as a function of flap deflection. The main effect of leading edge flap deflection is a partial suppression of the separated flow on the leeside of the wing. Qualitative comparison with experiments is presented, showing agreement in the general trends.

ACKNOWLEDGEMENT

This work was supported by NASA grant NCC 2-74

TABLE OF CONTENTS

NOMENCLATURE

Φ	perturbation velocity potential
Γ	vortex strength
α_i	exponent in the Schwarz-Christoffel transformation
α	angle of attack
ϵ	half apex angle of a main delta wing
δ	flap deflection angle
σ	coordinate of the physical plane
σ_v	vortex position in physical plane
η	coordinate of the transformed plane
η_v	vortex position in the transformed plane
η_i	tranformation coefficients
U	uniform velocity
F	complex potential
k	the ratio of the span length of the main wing to the total span length
U	uniform velocity
$\mathbf{n}$	normal vector of the flap surface
R	resultant force
R_w	resultant force on the main wing
R_F	resultant force on the flap surface
u, v, w	velocity components
C_L	lift coefficient
C_D	drag coefficient
C_p	pressure coefficient
C_N	normal force coefficient
ΔC_L	lift increment ; $C_{L\ flap} - C_{L\ without flap}$
N	normal force

1. INTRODUCTION

It is a well known phenomenon that above the leeside of a low aspect ratio delta wing at incidence there occurs a vortical flow originating from leading edges, and that this vortical flow is stable up to certain angle of attack. This vortical flow causes an enhancement of lift, called vortex lift, especially needed during maneuvering as well as in take-off and landing. Leading edge flaps have been suggested as a control device of this vortical flow to retain the necessary aircraft stability and control. This application of the leading edge flap is suitable for subsonic-transonic tactical delta wing aircraft, as well as aircraft having both supersonic cruise efficiency and high maneuverability.[1]

Coe and Weston[2] made experimental investigations on the effects of leading edge flaps. From their flow visualization it was found that leading edge deflection was effective in partly suppressing the formation of leading edge vortices and promoting attached flow condition. Hoffler and Rao[3] conducted experiments and theoretical studies using the vortex panel method, including the effect of tabbed flaps. Their results indicated an increase of lift-to-drag ratio. From the experimental results known so far we conclude that during flap deflection the drag is reduced considerably and the vortical flow is partially suppressed. The former contributes to an increase of lift-to-drag ratio and the latter causes a detrimental effect on lift. The second effect has been overcome by the use of flap tabs.[3,4,5]

Although many theoretical studies on the delta wing configuration have been conducted,[6,7,8,9] the flapped delta wing has not been analyzed outside the panel method context.[3] Moreover, the panel method does not provide a satisfactory explanation for the experimentally observed changes in the lift-to-drag ratio. In the present study we attempt to assess the trends of the effect of a leading edge flap on the aerodynamic characteristics of a slender delta wing. For mathematical convenience the conical geometry of the delta wing and the flap are chosen as shown in Fig. 1. The analysis is conducted in the cross-flow plane normal to the wing with the assumption that the flow field is also conical. For this purpose the simplest model for the separated flow[9] is chosen. This model is composed of a concentrated vortex and a straight vortex sheet, as shown in Fig. 2. In this model the analysis is carried out in a plane normal to the wing surface, which is

shown in Fig. 1. By means of a simple coordinate transformation the aerodynamic forces are resolved into lift and drag. A closed-form expression for the lift-to-drag ratio is found, which indicates that this ratio must increase with flap deflection. Comparison between theory and experiment shows generally similar trends for the aerodynamic coefficients.

2. MATHEMATICAL MODEL

2.1 Methodology

To study the qualitative trends of the effect of a leading edge flap on the aerodynamic characteristics of a low aspect ratio delta wing, the simplest model for the vortex sheet, suggested by Brown and Michael[9], is chosen. This model, as shown in Fig 2, simply assumes the rolled-up shear layer to consist of a straight vortex sheet and a singular vortex core and requires this singularity system to be force free in a global sence.

The trace of the wing in the cross-flow plane is transformed into the horizontal axis of the transformed plane by the Schwars-Christoffel tranformation. The advantage of this transformation is that the boundary condition on the wing surface is satisfied automatically in the mapping plane.

In this chapter the following effects of flap deflection are calculated and compared with experiments.[3]

- The influence of pressure forces acting on the flap surface on the lift-to-drag ratio.
- The drag on the main wing and the flap surface.
- The lift increment on the main wing and the flap surface.
- The influence of flap deflection angle on the vortex position and the force normal to the wing.

2.2 Analogy between 2-D unsteady flow and 3-D conica. flow

In this section a comparison between the three dimensional vortex sheet growing conically in space and the two dimensional vortex sheet growing in time is made. For the detailed mathematical procedure, refer to the paper by Küchmann and Weber.[6]

For an incompressible inviscid and irrotational flow the governing equation is

$$\nabla^2 \Phi = 0 \tag{1}$$

where Φ is the perturbation of the velocity potential due to the wing and the associated vortex sheets originating at the leading edges.

For a conical flow the perturbation of the velocity potential and the geometry of the vortex sheet can be written

$$\Phi(x,r,\theta) = x\,\phi(\bar{r},\theta) \tag{2}$$

$$S(x,r,\theta) = r - x\,f(\theta) \tag{3}$$

where $\bar{r} = r/x$ is the conical parameter.

In conical coordinates (1) becomes

$$\frac{1}{\bar{r}}\frac{\partial\phi}{\partial\bar{r}} + (1+\bar{r}^2)\frac{\partial^2\phi}{\partial\bar{r}^2} + \frac{1}{\bar{r}^2}\frac{\partial^2\phi}{\partial\theta^2} = 0 \quad . \tag{4}$$

The condition for the vortex sheet to be a streamline is

$$\mathbf{V}\cdot\nabla S = 0 \quad , \tag{5}$$

Combining (5) with (2) and (3) gives

$$\left(U+\phi-\bar{r}\frac{\partial\phi}{\partial\bar{r}}\right)f - \frac{\partial\phi}{\partial\bar{r}} + \frac{f'}{f}\frac{\partial\phi}{\partial\theta} = 0 \tag{6}$$

where $\phi - \bar{r}(\partial\phi/\partial\bar{r}) = v_x$.

The Bernoulli equation on the vortex sheet, postulating that no pressure difference across the vortex sheet exists, has the form

$$-\frac{p-p_0}{\rho/2} = 2U\left(\phi-\bar{r}\frac{\partial\phi}{\partial\bar{r}}\right) + \left(\phi-\bar{r}\frac{\partial\phi}{\partial\bar{r}}\right)^2 + \left(\frac{\partial\phi}{\partial\bar{r}}\right)^2 + \frac{1}{\bar{r}^2}\left(\frac{\partial\phi}{\partial\theta}\right)^2 \quad . \tag{7}$$

For an unsteady two dimensional flow, the potential function and the geometry of the vortex sheet can be written

$$\Phi(t,r,\theta) = \frac{R^2}{T}\left(\frac{t}{T}\right)^{2m-1}\phi(\bar{r},\theta) \tag{8}$$

$$S(t,r,\theta) = r - R\left(\frac{t}{T}\right)^m f(\theta) \tag{9}$$

where $\bar{r} = \left(\frac{r}{R}\right)\Big/\left(\frac{t}{T}\right)^m$ is Prandtl's unsteady similarity variable, and T and R are a characteristic time and length.[6]

For the unsteady case we finally have the velocity potential equation as

$$\frac{1}{\bar{r}}\frac{\partial\phi}{\partial\bar{r}} + \frac{\partial^2\phi}{\partial\bar{r}^2} + \frac{1}{\bar{r}^2}\frac{\partial^2\phi}{\partial\theta^2} = 0 \quad . \tag{10}$$

Boundary condition for the vortex sheet

$$m f - \frac{\partial\phi}{\partial\bar{r}} + \frac{f'}{f}\frac{\partial\phi}{\partial\theta} = 0 \quad . \tag{11}$$

Bernoulli equation for the vortex sheet

$$-\frac{p}{\rho/2} = \left(\frac{R}{T}\right)^2\left(\frac{t}{T}\right)^{2(m-1)}\left(2(2m-1)\phi - 2m\bar{r}\frac{\partial\phi}{\partial\bar{r}} + \left(\frac{\partial\phi}{\partial\bar{r}}\right)^2 + \frac{1}{\bar{r}^2}\left(\frac{\partial\phi}{\partial\theta}\right)^2\right) \quad . \tag{12}$$

Let's compare the velocity potential equation, the boundary condition and the Bernoulli equation on the vortex sheet for the unsteady case ((10),(11),(12)) with those of the conical case ((4),(6),(7)). First, the equations for the velocity potential in the two cases become identical if $\bar{r} \ll 1$. Next, the boundary condition and Bernoulli equation on the vortex sheet become equal if $m = 1$ and $v_x = \phi - \bar{r}(\partial\phi/\partial\bar{r}) \ll 1$. Finally we must get the relationship between x and t. This relationship can be obtained by returning the potential equation in both cases to the original variables. This gives

$$x\left(\frac{x^2}{r^2}\phi_{rr} + \frac{1}{r}\phi_r - 2\frac{x}{r}\phi_{xr} + \phi_{rr} + \frac{1}{r}\phi_r + + \frac{1}{r^2}\phi_{\theta\theta}\right) = 0 \tag{13}$$

$$t\left(\frac{t^2}{m^2r^2}\phi_{tt} - \frac{2-3m}{rm}\phi_r + \frac{1}{r^2}\frac{2m^2-3m+1}{m^2}\phi + \frac{t}{r^2}\frac{2-2m}{m^2}\phi_t - 2\frac{t}{r}\phi_{tr} + \right.$$

$$\left. \frac{1}{r^2}\phi_{\theta\theta} + \frac{1}{r}\phi_r + \phi_{rr}\right) = 0 \quad . \tag{14}$$

With $m = 1$ and $x = Ut$ these two equations become identical.

Now we see that the three dimensional conical flow could be calculated from the two dimensional unsteady flow if the following criteria were satisfied

(1) $\bar{r} \ll 1$, meaning that the flow is *geometrically slender.*

(2) $v_x \ll 1$, meaning that the flow is *aerodynamically slender*

If these two conditions are satisfied, we can solve the conical flow problem from a 2-D unsteady problem with the substitution of $x = Ut$ and $m = 1$.

The flow around a low aspect ratio delta wing satisfies these two conditions except near the vortex core, where v_x is close to U. Then, this analogy can be applied to slender delta wings with caution. Moreover, in concentrated vortex models, the axial velocity becomes singular at the core location, making the analogy more restrictive.

2.3 Vortex modelling

In the present model, composed of a straight vortex sheet and a singular vortex core as shown in Fig. 2, the vortex sheet and the vortex core do not follow streamlines; that is to say the vortex sheet and the vortex core are not independently force free. Thus, Joukowsky forces act both on the vortex sheet and the vortex core. In Brown and Michael's method these two forces are required to balance each other out, meaning that the whole system is force free.[9] Using the unsteady analogy derived in 2.2 and from Fig. 2c, we can find a force free condition for the whole vortex system. In the unsteady flow, the force free condition is

$$\rho U \, i\Gamma_i \left(\frac{d\sigma_{vi}}{dt} - V_{\sigma_{vi}} \right) + \rho \frac{d(i\Gamma_i)}{dt} (\sigma_{vi} - \sigma_{oi}) = 0 \quad , \tag{15}$$

where Γ_i is the i^{th} vortex strength,

σ_{vi} is the position of i^{th} vortex,

$V_{\sigma_{vi}}$ is the velocity at the i^{th} vortex position excluding its own induced velocity,

σ_{oi} is the origin of the straight vortex sheet

The first term is the force acting on the vortex core, the second is that acting on the vortex sheet. The term $d\sigma_{vi}/dt - V_{\sigma_{vi}}$ is the relative velocity causing the

Joukowsky force on the concentrated vortex core. The rate of change of the i^{th} vortex strength is $d(i\Gamma_i)/dt$ and this amount of vorticity is supplied through the straight vortex sheet having uniform strength, which connects the points from σ_{oi} to σ_{vi}.

From 2.2, the relationship between the 3-D conical flow and the 2-D unsteady flow is

$$\frac{d}{dt} = U\frac{d}{dx} \tag{16}$$

and from the geometry of a delta wing, the conical relationship gives

$$k = x\epsilon \tag{17a}$$

$$\frac{d\Sigma}{dx} = \frac{\Sigma}{x} = \frac{\epsilon}{k}\Sigma \tag{17b}$$

where Σ stands for any quantity associated with the kinematics of the flow field, and k is defined in Fig. 3 and ϵ is the half apex angle of the main delta wing. Then the force free condition on the i^{th} vortex system can be rewritten

$$\frac{U\epsilon}{k}(2\sigma_{vi} - \sigma_{oi}) = V_{\sigma_{vi}} \tag{18a}$$

$$\overline{V}_{\sigma_{vi}} = \frac{d}{d\sigma}\left(F - \frac{i\Gamma_i}{2\pi}\log(\sigma - \sigma_{vi})\right) \quad . \tag{18b}$$

where F is the total complex potential of the flow field.

In our case we have a system of four vortices fed by vortex sheets emanating from the leading edges and from the flap junctions. Since only the symmetrical configurations are treated, the analysis considers one half of the cross flow plane. Thus $\sigma_{o1} = i\,(k + (1-k)e^{i\delta})$ for the leading edge vortex and $\sigma_{o2} = i\,k$ for the flap junction vortex. Then the force free conditions for both vortex systems are

$$\frac{U\epsilon}{k}\left(2\overline{\sigma}_{v1} + i(k + (1-k)e^{-i\delta})\right) = \frac{d}{d\sigma}\left(F - \frac{i\Gamma_1}{2\pi}\log(\sigma - \sigma_{v1})\right)\Big|_{\sigma\to\sigma_{v1}} \tag{19}$$

$$\frac{U\epsilon}{k}\left(2\bar{\sigma}_{v2}+ik\right) = \frac{d}{d\sigma}\left(F - \frac{i\Gamma_2}{2\pi}log(\sigma-\sigma_{v2})\right)\Big|_{\sigma=\sigma_{v2}} \quad . \tag{20}$$

The derivation of the complex potential is facilitated by transforming the trace of the wing, together with its line of symmetry, into the real axis of a transformed plane. To perform this transformation the Schwarz-Christoffel transformation is used. The mapping procedure is shown in Fig. 3.

The general form of Scwarz-Christoffel transformation is

$$\frac{d\sigma}{d\eta} = A\prod_{i=1}^{n}(\eta-\eta_i)^{\alpha_i} \quad , \tag{21}$$

In integral form

$$\sigma = C + A\int_{\eta_o}^{\eta}\prod_{i=1}^{n}(\eta-\eta_i)^{\alpha_i}\,d\eta \quad , \tag{22}$$

where $\alpha_i = k_i/\pi - 1$, k_i is the angle at the i^{th} vertex of the polygon, and η_i is the corresponding point of σ in the mapping plane. A and C are complex constants.

From Fig. 3, we get

$$k_1 = \pi \ , \ k_2 = \pi/2 \ , \ k_3 = \pi - \delta \ , \ k_4 = 2\pi \ , \ k_5 = \pi + \delta \ , \ k_6 = \pi/2 \quad , \tag{23}$$

then

$$\alpha_1 = 0 \ , \ \alpha_2 = -1/2 \ , \ \alpha_3 = -\delta/\pi \ , \ \alpha_4 = 1 \ , \ \alpha_5 = \delta/\pi \ , \ \alpha_6 = -1/2 \quad . \tag{24}$$

From Riemann's mapping theorem we can arbitrarily choose two points. Let these two points be

$$\eta_1 = 0 \tag{25a}$$

$$\eta_o = \eta_2 \tag{25b}$$

These conditions imply that the leading edge is transformed to the origin and the initial point of the integration is taken arbitrarily at η_2. Requiring that the velocity in both planes be equal at infinity, we have

$$\left.\frac{d\sigma}{d\eta}\right|_{\sigma\to\infty} = 1 \quad . \tag{26}$$

With (25) and (26), the transformation function becomes

$$\sigma = \int_{\eta_2}^{\eta} \frac{\eta}{\sqrt{(\eta-\eta_2)(\eta-\eta_3)}} \left(\frac{\eta-\eta_5}{\eta-\eta_3}\right)^{\delta/\pi} d\eta \quad . \tag{27}$$

The constants η_2, η_3, η_5, η_6 can be obtained by matching the four corresponding points in the physical and the transformed plane

$$\sigma_3 = ik \quad \rightarrow \quad \eta_3 \tag{28a}$$

$$\sigma_4 = ik(1+(1-k)e^{i\delta}) \quad \rightarrow \quad 0 \tag{28b}$$

$$\sigma_5 = ik \quad \rightarrow \quad \eta_5 \tag{28c}$$

$$\sigma_6 = 0 \quad \rightarrow \quad \eta_6 \quad . \tag{28d}$$

Here lengths are normalized with the half span length $a(x)$.
Applying (28),

$$k + \int_{\eta_2}^{\eta_3} \frac{\xi}{\sqrt{(\eta_6-\xi)(\xi-\eta_2)}} \left(\frac{\eta_5-\xi}{\eta_3-\xi}\right)^{\delta/\pi} d\xi = 0 \tag{29a}$$

$$1-k + \int_{\eta_3}^{0} \frac{\xi}{\sqrt{(\eta_6-\xi)(\xi-\eta_2)}} \left(\frac{\eta_5-\xi}{\xi-\eta_3}\right)^{\delta/\pi} d\xi = 0 \tag{29b}$$

$$1-k - \int_{0}^{\eta_3} \frac{\xi}{\sqrt{(\eta_6-\xi)(\xi-\eta_2)}} \left(\frac{\eta_5-\xi}{\xi-\eta_3}\right)^{\delta/\pi} d\xi = 0 \tag{29c}$$

$$k - \int_{\eta_5}^{\eta_6} \frac{\xi}{\sqrt{(\eta_6-\xi)(\xi-\eta_2)}} \left(\frac{\xi-\eta_5}{\xi-\eta_3}\right)^{\delta/\pi} d\xi = 0 \quad . \tag{29d}$$

This system is solved numerically for η_2, η_3, η_5, η_5 as shown in Appendix 1.

From Fig. 3 we see that the complex potential in the transformed plane is the sum of the potentials of a unform velocity and that of four vortices, two of which are the image vortex systems needed to satisfy the boundary condition on the wing surface. Here we neglect the influence of the vortex sheet on the flow field.

Then the complex potential in mapping plane is

$$F(\eta) = U\alpha\eta + \frac{i\Gamma_1}{2\pi}log\left(\frac{\eta-\eta_{v1}}{\eta-\bar{\eta}_{v1}}\right) - \frac{i\Gamma_2}{2\pi}log\left(\frac{\eta-\eta_{v2}}{\eta-\bar{\eta}_{2v}}\right) \quad , \tag{30}$$

and the complex velocity in the physical plane is

$$\begin{aligned}\frac{dF}{d\sigma} &= \frac{dF}{d\eta}\frac{d\eta}{d\sigma} \\ &= \left[U\alpha + \frac{i\Gamma_1}{2\pi}\left(\frac{1}{\eta-\eta_{v1}} - \frac{1}{\eta-\bar{\eta}_{v1}}\right) - \frac{i\Gamma_2}{2\pi}\left(\frac{1}{\eta-\eta_{v2}} - \frac{1}{\eta-\bar{\eta}_{v2}}\right)\right]\frac{d\eta}{d\sigma}\end{aligned} \quad , \tag{31}$$

where

$$\frac{d\eta}{d\sigma} = \frac{\sqrt{(\eta-\eta_3)(\eta-\eta_2)}}{\eta}\left(\frac{\eta-\eta_3}{\eta-\eta_5}\right)^{\delta/\pi} \quad . \tag{32}$$

According to (32) the velocity becomes singular at the leading edge, $\eta = 0$, and at the flap junction, $\eta = \eta_5$. To avoid this singularity we apply the Kutta condition at these two points. The two equations for the Kutta condition are

$$U\alpha + \frac{i\Gamma_1}{2\pi}\left(\frac{1}{\bar{\eta}_{v1}} - \frac{1}{\eta_{v1}}\right) - \frac{i\Gamma_2}{2\pi}\left(\frac{1}{\bar{\eta}_{v2}} - \frac{1}{\eta_{v2}}\right) = 0 \quad , \tag{33}$$

$$U\alpha + \frac{i\Gamma_1}{2\pi}\left(\frac{1}{\eta_5-\eta_{v1}} - \frac{1}{\eta_5-\bar{\eta}_{v1}}\right) - \frac{i\Gamma_2}{2\pi}\left(\frac{1}{\eta_5-\eta_{v2}} - \frac{1}{\eta_5-\bar{\eta}_{v2}}\right) = 0 \quad . \tag{34}$$

With the complex potential F the force free conditions given by (19) and (20)

become

$$\frac{U\epsilon}{k}\Big(2\bar{\sigma}_{v1}+i(k+(1-k)e^{-i\delta}\Big) =$$

$$\left[U\alpha - \frac{i\Gamma_1}{2\pi}\frac{1}{\eta_{v1}-\bar{\eta}_{v1}} - \frac{i\Gamma_2}{2\pi}\left(\frac{1}{\eta_{v1}-\eta_{v2}} - \frac{1}{\eta_{v1}-\bar{\eta}_{v2}}\right)\right]\times$$

$$\left(\frac{\sqrt{(\eta_{v1}-\eta_6)(\eta_{v1}-\eta_2)}}{\eta_{v1}}\left(\frac{\eta_{v1}-\eta_3}{\eta_{v1}-\eta_5}\right)^{\delta/\pi}\right) \qquad (35)$$

$$+\frac{i\Gamma_1}{2\pi}\frac{d}{d\sigma}\Big[log(\eta-\eta_{v1}) - log(\sigma-\sigma_{v1})\Big]_{\sigma\to\sigma_{v1}}$$

$$\frac{U\epsilon}{k}\Big(2\bar{\sigma}_{v2}+ik\Big) =$$

$$\left[U\alpha - \frac{i\Gamma_1}{2\pi}\left(\frac{1}{\eta_{v2}-\eta_{v1}} - \frac{1}{\eta_{v2}-\bar{\eta}_{v1}}\right) + \frac{i\Gamma_2}{2\pi}\frac{1}{\eta_{v2}-\bar{\eta}_{v2}}\right]\times$$

$$\left(\frac{\sqrt{(\eta_{v2}-\eta_6)(\eta_{v2}-\eta_2)}}{\eta_{v2}}\left(\frac{\eta_{v2}-\eta_3}{\eta_{v2}-\eta_5}\right)^{\delta/\pi}\right) \qquad (36)$$

$$-\frac{i\Gamma_2}{2\pi}\frac{d}{d\sigma}\Big[log(\eta-\eta_{v2}) - log(\sigma-\sigma_{v2})\Big]_{\sigma\to\sigma_{v2}}$$

Combining (33) and (34) with (35) and (36), we get the following two complex equations for the vortex positions.

$$\frac{\epsilon}{k\alpha}\left(2\bar{\sigma}_{v1} + i\Big(k+(1-k)e^{-i\delta}\Big)\right) =$$

$$\left[1 - \frac{D-B}{CB-AD}\frac{1}{\eta_{v1}-\bar{\eta}_{v1}} - \frac{C-A}{CB-AD}\left(\frac{1}{\eta_{v1}-\eta_{v2}} - \frac{1}{\eta_{v1}-\bar{\eta}_{v2}}\right)\right]\times \qquad (37)$$

$$\left(\frac{d\sigma}{d\eta}\right)\Big|_{\sigma=\sigma_{v1}} + \frac{D-B}{CB-AD}\frac{d}{d\sigma}\Big(log(\eta-\eta_1) - log(\sigma-\sigma_{v1})\Big)\Big|_{\sigma\to\sigma_{v1}}$$

$$\frac{\epsilon}{k\alpha}\,(2\bar{\sigma}_{v2}+ik)=$$

$$\left[1+\frac{D-B}{CB-AD}\left(\frac{1}{\eta_{v2}-\eta_{v1}}-\frac{1}{\eta_{v2}-\bar{\eta}_{v1}}\right)+\frac{C-A}{CB-AD}\,\frac{1}{\eta_{v2}-\bar{\eta}_{v2}}\right]\times \quad , \qquad (38)$$

$$\left(\frac{d\sigma}{d\eta}\right)\Big|_{\sigma=\sigma_{v2}}+\frac{A-C}{CB-AD}\,\frac{d}{d\sigma}\Big(log(\eta-\eta_{v2})-log(\sigma-\sigma_{v2})\Big)\Big|_{\sigma\to\sigma_{v2}}$$

where

$$A=\frac{1}{\bar{\eta}_{v1}}-\frac{1}{\eta_{v1}} \qquad (39a)$$

$$B=\frac{1}{\bar{\eta}_{v2}}-\frac{1}{\eta_{v2}} \qquad (39b)$$

$$C=\frac{1}{\eta_5-\eta_{v1}}-\frac{1}{\eta_5-\bar{\eta}_{v1}} \qquad (39c)$$

$$D=\frac{1}{\eta_5-\eta_{v2}}-\frac{1}{\eta_5-\bar{\eta}_{v2}} \quad . \qquad (39d)$$

In the absence of flaps the only governing parameter would be the ratio of ϵ/α . In the present case two additional parameters ,δ and k, are included in the group $\epsilon/(k\ \alpha)$. The flap deflection angle δ does not appear explicitly but through the transformation parameters η_2, η_3, η_5 and η_6, which are functions of δ and k.

A Newton-Raphson meth d is used to solve the above two equations, the detailed numerical procedure is given in Appendix 2.

With the vortex positions known we get the vortex strengths from

$$\frac{i\,\Gamma_1}{2\pi}=\frac{D-B}{CB-AD}\,U\alpha \qquad (40a)$$

$$\frac{i\,\Gamma_2}{2\pi}=\frac{C-A}{CB-AD}\,U\alpha \quad . \qquad (40b)$$

2.4 Aerodynamic forces

2.4.1 Resultant force

To calculate the resultant force on each surface we consider the pressure coefficient.

$$C_p = 1 + \alpha^2 - (u/U)^2 - (v/U)^2 - (w/U)^2 \quad , \tag{41}$$

where the v and w components are given by

$$v = \frac{\partial \Phi}{\partial y} \tag{42a}$$

$$= \mathrm{Re}\left(\frac{\partial F}{\partial y}\right) \tag{42b}$$

$$= \mathrm{Re}\left(V \frac{\partial \sigma}{\partial y}\right) \tag{42c}$$

$$= \mathrm{Re}\left[\left(U\alpha + \frac{i\Gamma_1}{2\pi}\left(\frac{1}{\eta - \eta_{v1}} - \frac{1}{\eta - \bar{\eta}_{v1}}\right) - \frac{i\Gamma_2}{2\pi}\left(\frac{1}{\eta - \eta_{v2}} - \frac{1}{\eta - \bar{\eta}_{v2}}\right)\right) \times \left(\frac{\sqrt{(\eta - \eta_6)(\eta - \eta_2)}}{\eta}\left(\frac{\eta - \eta_3}{\eta - \eta_5}\right)^{\delta/\pi}\right)\right] \quad , \tag{42d}$$

$$w = \frac{\partial \Phi}{\partial z} \tag{43a}$$

$$= \mathrm{Re}\left(\frac{\partial F}{\partial \eta}\,\frac{d\eta}{d\sigma}\,\frac{\partial \sigma}{\partial z}\right) \tag{43b}$$

$$= \mathrm{Re}\,(i\,V) \tag{43c}$$

here $\sigma = y + i\,z$ and $V = (\partial F/\partial \eta)(\partial \eta/\partial \sigma)$ i.e. the complex velocity in the cross-flow plane.

The u component is best obtained from the conical flow condition

$$u = U + \frac{1}{x}\left(\Phi - y\frac{\partial \Phi}{\partial y} - z\frac{\partial \Phi}{\partial z}\right) \tag{44a}$$

$$= U + \frac{\epsilon}{k}\,\mathrm{Re}\left[U\alpha\eta + \frac{i\Gamma_1}{2\pi}\log\left(\frac{\eta - \eta_{v1}}{\eta - \bar{\eta}_{v1}}\right) - \frac{i\Gamma_2}{2\pi}\log\left(\frac{\eta - \eta_{v2}}{\eta - \bar{\eta}_{v2}}\right) - yv - zw\right] \tag{44b}$$

The presence of the feeding sheet induces a discontinuity in the u component of the velocity, as demonstrated in Appendix 3.

The resultant force is given by

$$R = \int_{each\ surface} p\, d\sigma \tag{45}$$

This integration is carried out numerically in the physical plane.

2.4.2 Lift-to-Drag ratio

Most experiments[2,3,5] show an increase of lift-to-drag ratio with flap deflection. Before we calculate the lift-to-drag ratio we must consider the normal vector on the flap surface. The rotation of the leading edge flap about the flap hinge axis causes the normal vector to have a component opposite to the free stream. Associated with this component there is a force tending to decrease the drag, which is responsible for the increase in C_L/C_D . This component can be obtained by performing the following transformations:

Let's take the longitudinal axis of the wing as x, the axis normal to the wing surface as y and the starboard direction as $-z$, as shown in Fig. 1. e_x, e_y, e_z denote the unit vectors along axis x, y, z . With the rotations shown in Fig. 4, these vectors are expressed as

$$\begin{pmatrix} e_{x_1} \\ e_{y_1} \\ e_{z_1} \end{pmatrix} = \begin{pmatrix} \cos\epsilon & 0 & \sin\epsilon \\ 0 & 1 & 0 \\ -\sin\epsilon & 0 & \cos\epsilon \end{pmatrix} \begin{pmatrix} e_x \\ e_y \\ e_z \end{pmatrix} \tag{46}$$

$$\begin{pmatrix} e_{x_2} \\ e_{y_2} \\ e_{z_2} \end{pmatrix} = \begin{pmatrix} 1 & 0 & 0 \\ 0 & \cos\delta & \sin\delta \\ 0 & -\sin\delta & \cos\delta \end{pmatrix} \begin{pmatrix} e_{x_1} \\ e_{y_1} \\ e_{z_1} \end{pmatrix} . \tag{47}$$

Identifying n with the normal vector to the flap surface we have

$$\mathbf{n} = e_{y_2} . \tag{48}$$

Then

$$\begin{aligned} \mathbf{n} &= \cos\delta\, \mathbf{e}_{y_1} + \sin\delta\, \mathbf{e}_{z_1} \\ &= \cos\delta\, \mathbf{e}_{y_1} + \sin\delta(-\sin\epsilon\, \mathbf{e}_x + \cos\epsilon\, \mathbf{e}_z) \\ &\simeq -\epsilon\sin\delta\, \mathbf{e}_x + \cos\delta\, \mathbf{e}_y + \sin\delta\, \mathbf{e}_z \end{aligned} \tag{49}$$

The first term in the last line shows the forward component of the normal vector. This term contributes to the increase of the lift-to-drag ratio when the flap is deflected. The first component, $-\epsilon\sin\delta$, gives the thrust force and is of higher order than the other two. As the flap is deflected the vortex comes closer to the wing surface, causing a considerable change in drag.

On the main wing the resultant force is normal to the wing surface. Then the lift and the drag components are

$$L_w = R_w \tag{50a}$$

$$D_w = R_w\,\alpha \tag{50b}$$

where R_w is the resultant force on the main wing.

On the flap surface there are all three components of force, as indicated by (49)

$$R_{Fx} = -R_F\,\epsilon\sin\delta \tag{51a}$$

$$R_{Fy} = R_F\cos\delta \tag{51b}$$

$$R_{Fz} = R_F\,\epsilon\sin\delta \tag{51c}$$

where R_F is the resultant force on the flap surface.

Since the R_{Fz} component is cancelled by symmetry, only R_{Fx} and R_{Fy} contribute to lift and drag

$$L_F = R_{Fy} - R_{Fx}\,\alpha \tag{52a}$$

$$D_F = R_{Fy}\,\alpha + R_{Fx}\cos\delta \quad . \tag{52b}$$

From (51a) and (51b)

$$R_{Fx} = -\epsilon\tan\delta\, R_{Fy} \quad . \tag{53}$$

From (51),(52) and (53) we get the drag and lift on the flap

$$L_F = R_{Fy}\,(1+\epsilon\,\alpha\,tan\delta) \tag{54a}$$

$$D_F = \alpha\,R_{Fy}\left(1-\frac{\epsilon}{\alpha}\,tan\delta\right) \tag{54b}$$

The total lift and drag are

$$L = R_w + R_{Fy}(1+\epsilon\,\alpha\,tan\delta) \tag{55}$$

$$D = \alpha\left(R_w + R_{Fy}\left(1-\frac{\epsilon}{\alpha}\,tan\delta\right)\right) \quad . \tag{56}$$

(55) and (56) show the influence of the forward component of force on the lift and the drag. Due to this thrust component the lift increases by an amount of order α^2, while the drag is reduced by almost the same order as the drag itself. This increases the lift-to-drag ratio during flap deflection.

For moderate deflection angle the lift-to-drag ratio is

$$\frac{L}{D} = \frac{1}{\alpha}\left[\left(1+\frac{R_{Fy}}{R_w+R_{Fy}}\frac{\epsilon}{\alpha}tan\,\delta\right)+O(\alpha^2)\right]. \tag{57}$$

Numerical results show that the lift itself also decreases with flap deflection while the lift-to-drag ratio increases.

2.4.3 Normal force

As mentioned in the previous section the lift decreases with flap deflection. By considering the normal force we can infer the reason for this reduction.

The normal force can be calculated by considering the momentum change in the cross-flow plane

$$N = -\rho U\int\int\left(\frac{\partial\Phi}{\partial y}-U\alpha\right)dydz \tag{58}$$

Applying Stokes' theorem

$$N = -\rho U\int_c \Phi\,dz \tag{59}$$

In terms of the complex potential and the real stream function

$$N = -\rho U \int_c \mathrm{Im}\,(F\,d\sigma - i\,\Psi\,d\sigma) \tag{60}$$

Since the contour is a streamline

$$N = -\rho U \int_c \mathrm{Im}\,(F\,d\sigma) \tag{61}$$

Substituting for F

$$N = -\rho U \mathrm{Im} \int_c \left(U\alpha\eta + \frac{i\Gamma_1}{2\pi} log\left(\frac{\eta-\eta_{v1}}{\eta-\overline{\eta}_{v1}}\right) - \frac{i\Gamma_2}{2\pi} log\left(\frac{\eta-\eta_{v2}}{\eta-\overline{\eta}_{v2}}\right)\right) \frac{d\sigma}{d\eta}\, d\eta \tag{62}$$

To perform this integral we first express the part containing the logarithmic terms on a circle of infinite radius, where $d\sigma/d\eta = 1$

$$\begin{aligned} &\int_c \left(\frac{i\Gamma_1}{2\pi} log\left(\frac{\eta-\eta_{v1}}{\eta-\overline{\eta}_{v1}}\right) - \frac{i\Gamma_2}{2\pi} log\left(\frac{\eta-\eta_{v2}}{\eta-\overline{\eta}_{v2}}\right)\right)\frac{d\sigma}{d\eta} d\eta \\ &= \int_{r=\infty} \left(\frac{i\Gamma_1}{2\pi} log\left(\frac{\eta-\eta_{v1}}{\eta-\overline{\eta}_{v1}}\right) - \frac{i\Gamma_2}{2\pi} log\left(\frac{\eta-\eta_{v2}}{\eta-\overline{\eta}_{v2}}\right)\right) d\eta \quad . \end{aligned} \tag{63}$$

We see that in the transformed plane the normal force arising from the logarithmic terms does not depend explicitly on the wing trace, but implicitly through the vortices positions and strengths. This equation shows that the normal force is just the sum of the rate change of impulse of two pairs of vortices. Then the result could be simply obtained by considering the impulse of a pair vortices, or by integrating around the vortex sheet as shown in Fig. 5a. Following this second approach gives

$$\begin{aligned} &\int_{r=\infty} \frac{i\Gamma_1}{2\pi}\Big(log(\eta-\eta_{v1}) - log(\eta-\overline{\eta}_{v1})\Big)\, d\eta \\ &= \frac{i\Gamma_1}{2\pi}\left[\int_{\overline{\eta}_{v1}}^{\eta_{v1}} log(\eta-\eta_{v1})|_p - log(\eta-\overline{\eta}_{v1})|_p - i\,2\pi\, d\eta \right. \\ &\qquad \left. + \int_{\eta_{v1}}^{\overline{\eta}_{v1}} log(\eta-\eta_{v1})|_p - log(\eta-\overline{\eta}_{v1})|_p\, d\eta\right] \\ &= \Gamma_1\,(\eta_{v1} - \overline{\eta}_{v1}) \quad . \end{aligned} \tag{64}$$

Then the normal force originating from the logarithmic terms is

$$N_c = \mathrm{Im}\ \rho U[\,\Gamma_1(\eta_{v1} - \bar{\eta}_{v1}) - \Gamma_2(\eta_{v2} - \bar{\eta}_{v2})] \quad . \tag{65}$$

This force is associated with the separated flow field about the wing.

The component of normal force from the the first term in (62) has a singularity at infinity. This component could be identified with the force produced by the wing if the flow were attached. Integrating along the wing trace, as shown in Fig. 5b, we find

$$\begin{aligned}
&\int_c \frac{\eta^2}{\sqrt{(\eta-\eta_6)(\eta-\eta_2)}}\left(\frac{\eta-\eta_5}{\eta-\eta_3}\right)^{\delta/\pi} d\eta \\
&= \int_{\eta_2}^{\eta_3} \frac{\eta^2}{\sqrt{(\eta-\eta_6)(\eta-\eta_2)}}\bigg|_p \left(\frac{\eta-\eta_5}{\eta-\eta_3}\right)^{\delta/\pi}\bigg|_p d\eta \\
&+ \int_{\eta_3}^{\eta_3} \frac{\eta^2}{\sqrt{(\eta-\eta_6)(\eta-\eta_2)}}\bigg|_p \left(\frac{\eta-\eta_5}{\eta-\eta_3}\right)^{\delta/\pi}\bigg|_p \frac{1}{e^{i2\delta}}\, d\eta \\
&+ \int_{\eta_3}^{\eta_6} \frac{\eta^2}{\sqrt{(\eta-\eta_6)(\eta-\eta_2)}}\bigg|_p \left(\frac{\eta-\eta_5}{\eta-\eta_3}\right)^{\delta/\pi}\bigg|_p \frac{e^{i2\delta}}{e^{i2\delta}}\, d\eta \\
&+ \int_{\eta_6}^{\eta_3} - \frac{\eta^2}{\sqrt{(\eta-\eta_6)(\eta-\eta_2)}}\bigg|_p \left(\frac{\eta-\eta_5}{\eta-\eta_3}\right)^{\delta/\pi}\bigg|_p \frac{e^{i2\delta}}{e^{i2\delta}}\, d\eta \\
&+ \int_{\eta_3}^{\eta_3} - \frac{\eta^2}{\sqrt{(\eta-\eta_6)(\eta-\eta_2)}}\bigg|_p \left(\frac{\eta-\eta_5}{\eta-\eta_3}\right)^{\delta/\pi}\bigg|_p \frac{e^{i4\delta}}{e^{i2\delta}}\, d\eta \\
&+ \int_{\eta_3}^{\eta_2} - \frac{\eta^2}{\sqrt{(\eta-\eta_6)(\eta-\eta_5)}}\bigg|_p \left(\frac{\eta-\eta_5}{\eta-\eta_3}\right)^{\delta/\pi}\bigg|_p \frac{e^{i4\delta}}{e^{i4\delta}}\, d\eta \\
&= 2\left(\int_{\eta_2}^{\eta_3} + \int_{\eta_5}^{\eta_6} + \cos 2\delta \int_{\eta_3}^{\eta_5}\right) \frac{\eta^2}{\sqrt{(\eta-\eta_6)(\eta-\eta_2)}}\bigg|_p \left(\frac{\eta-\eta_5}{\eta-\eta_3}\right)^{\delta/\pi}\bigg|_p d\eta
\end{aligned} \tag{66}$$

where subscript p represents the principal value that means all values must be calcualted in the same Riemann surface.

Then the total normal force is

$$N = \mathrm{Im}\left(\rho U\,\Gamma_1(\eta_{v1} - \bar{\eta}_{v1}) - \rho U\,\Gamma_2(\eta_{v2} - \bar{\eta}_{v2})\right)$$
$$- \rho U^2\,\alpha\,\mathrm{Im}\int_c \frac{\eta^2}{\sqrt{(\eta-\eta_6)(\eta-\eta_2)}}\left(\frac{\eta-\eta_5}{\eta-\eta_3}\right)^{\delta/\pi} d\eta \qquad (67)$$

The normal force is composed of two parts; the normal force from equivalent attached flow and that from the separated flow.

Dividing this total normal force by the dynamic pressure $\rho U^2/2$ and the projected area $k\,a(x)\,(k+(1-k)\cos\delta)/\epsilon$, we get the normal force coefficient

$$C_N = \frac{\epsilon}{k}\,\frac{1}{k+(1-k)\cos\delta}\times$$
$$\mathrm{Im}\Big[2\Gamma_1(\eta_{v1} - \bar{\eta}_{v1}) - 2\Gamma_2(\eta_{v2} - \bar{\eta}_{v2}) -$$
$$4\alpha\left(\left(\int_{\eta_2}^{\eta_3} + \int_{\eta_3}^{\eta_6} + \cos 2\delta \int_{\eta_3}^{\eta_5}\right)\frac{\eta^2}{\sqrt{(\eta-\eta_6)(\eta-\eta_2)}}\left(\frac{\eta-\eta_5}{\eta-\eta_3}\right)^{\delta/\pi}\Big|_p d\eta\right)\Big] \qquad (68)$$

where the vortex intensity and η have been normalised with $U\,a(x)$ and $a(x)$ respectively.

Here all the values of the integrand are the principal values. This shows explicitly the effect of the flap angle on the normal force. The region from η_3 to η_5 is the flap surface.

For flap deflection angles much larger than the angle of attack, it is conceivable that the vortex may be located underneath the wing surface.[6] In this case the dominant component in the cross flow plane is not $U\,\alpha$ but the projection of U on a plane normal to the flap surface. This fact imposes a limit to the flap angles for which this theory is expected to apply.

3. RESULTS AND CONCLUSIONS

3.1 Results

3.1.1 Conformal mapping

The following table shows the transformation coefficients η_2, η_3, η_4 and a_5 for varying flap deflection angle δ, with $b = 0.6$ and $\epsilon = 15.95°$.

δ(deg.)	η_2	η_3	η_5	η_6
40.	−0.6369	−0.5160	0.9785	1.301
36.	−0.6729	−0.5441	0.9659	1.277
32.	−0.7091	−0.5722	0.9513	1.251
28.	−0.7456	−0.6004	0.9355	1.223
24.	−0.7824	−0.6284	0.9183	1.192
20.	−0.8191	−0.6562	0.8997	1.165
16.	−0.8553	−0.6833	0.8794	1.134
12.	−0.8924	−0.7105	0.8583	1.102
8.	−0.9286	−0.7371	0.8362	1.069
4.	−0.9644	−0.7629	0.8130	1.035
2.	−0.9822	−0.7755	0.8010	1.018

Table I

We see that as $\delta \to 0$, $\eta_2 \to -1$ and $\eta_3 \to 1$, which correspond to the Brown and Michael case.

3.1.2 Aerodynamic forces

To compare with the experimental results of ref. [3] a wing with $\epsilon = 15.95°$ and $b = 0.6$ is chosen. The angle of attack is varied from $0°$ to $20°$.

Fig. 6 shows the contribution to the drag of the main wing. It can be seen that the model overestimates the drag, particularly at higher angles of attack.

Fig. 7 shows the contribution to the drag of the flap. Notice that this component of drag can reach negative values. This is due to the forward force component discussed above.

Fig. 8 and 9 show the increment of lift on the main wing and flap respectively. The abrupt departure from experiments observed at about 12^o appears to suggest vortex breakdown in the experiments.

Fig. 10 shows the evolution of the resultant drag. The negative values of drag arise from the conical assumptions, where no trailing vortices and associated drag are considered.

Fig. 11 depicts the total lift change. Again, the sudden departure from the experimental trends may indicate that those measurements were affected by vortex breakdown.

Fig. 12 shows the change in the C_L/C_D ratio. No experimental values were available. The no-deflection case is included for comparison.

Fig. 13 shows the positions of vortices for varying flap deflection. For flap deflections less than 16^o the secondary vortex almost disappears. The vortex positions in the physical plane are shown in Fig. 14. We notice that flap deflection causes the secondary vortex to move away from the surface and the leading edge vortex to approach the surface.

Fig. 15 describes the strength of both vortices as function of flap deflection. Flap deflection strengthens the secondary vortex and weakens the leading edge vortex. The strength of leading edge vortex reduces by a half in 40^o flap deflection.

Fig. 16 shows the different components of normal force. We notice that flap deflection acts primarily on the leading edge vortex component of the normal force. The secondary vortex has a negligible effect on the total force.

3.2 Conclusions

A conical delta wing with leading edge flaps was analyzed using a simple vortex-feeding-sheet model consisting of two pairs of vortices with corresponding vortex sheets. One pair originates at the leading edges and the other at the flap junctions. The leading edge vortex pair is much stronger and responsible for most of the lift and drag changes that take place during flap deflection. In agreement with experimental evidence, it was found that flap deflection causes a decrease of lift and drag, and an increase of the lift-to-drag ratio. A closed form expression exhibiting the lift-to-drag ratio increase was derived. The rapid reduction in drag is attributable to a thrust

force component developed by the flaps, while the main reason for the lift reduction is the partial suppression of the vortical flow. There is agreement with experiments in the general trends.

The two main sources of limitation of the theory are the crudness of the vortex system representation, and the assumption that a cross-flow plane can be suitably defined. The latter aspect becomes relevant in highly warped wings, which in this case amounts to flap deflections that are large and comparable to the angle of attack, where the notion of a plane normal to the wing becomes meaningless.

References

1. J.E. Lamar and J.F. Campbell, " Vortex Flaps - Advanced Control Devices for Supercruise Fighters ", Aerospace America, Jan., 1984
2. P.L. Coe, Jr. and R.P. Weston, " Effects of Wing Leading-Edge Deflection on Low-Speed Aerodynamic Chracteristics of a Low-Aspect- Ratio Highly Swept Arrow-Wing Cinfiguration ", NASA TP 1434, 1979
3. K.D. Hoffler and D.M. Rao, " An Investigation of the Tabbed Vortex Flap ", J. Aircraft, Vol. 22, No. 6, pp 490-497, 1985
4. D.M. Rao, " Vortical Flow Management for Improved Configuration Aerodynamics - Recent Experiences ", AGARD CP 342, 1983
5. L.P. Yip and D.G. Murri, " Effect of Vortex Flaps on the Low-Speed Aerodynamics of an Arrow Wing ", NASA TP 1914, 1981
6. D.Küchmann and J. Webber, "Vortex Motions", Zeithschrift Für Angewandte Mathematik und Mechanik, 45, pp 457 - 474, 1965
7. D. Küchmann, The Aerodynamic Design of Aircraft , Pergamon press, 1979
8. R.T. Jones, " Properties of Low-Aspect-Ratio Pointed Wings at Speeds below and above the Speed of Sound ", NACA Rep. No. 835, 1946
9. C.E. Brown and W.H. Michael, Jr., " On Slender Delta Wings with Leading-Edge Separation ", NACA TN 3430, 1955

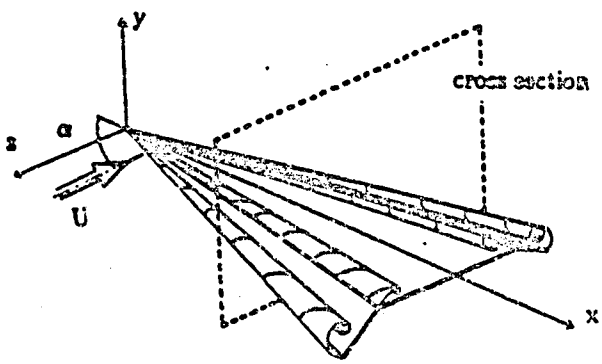

Fig. 1. Overview of the assumed flow field.

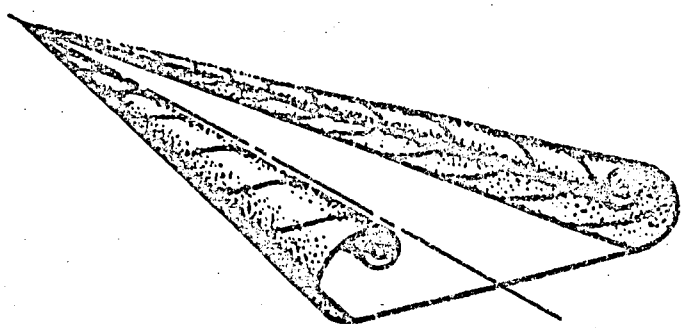

(a) assumed flow field

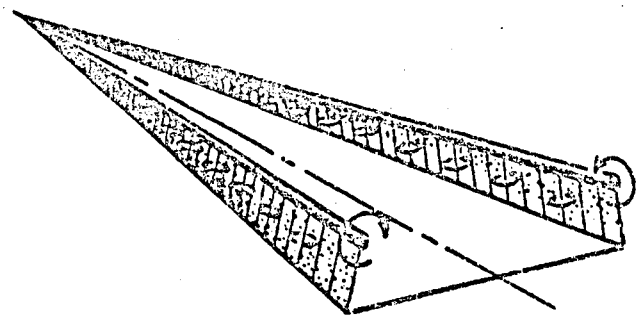

(b) approximated flow field

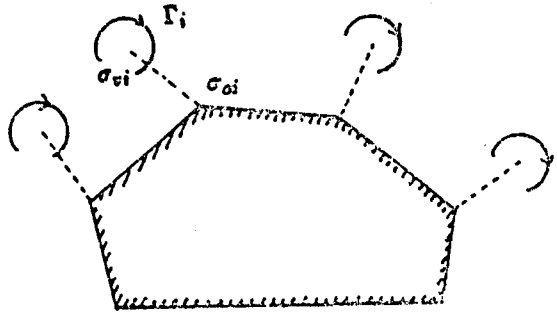

(c) Vortex system with straight feeding sheets

Fig. 2. Brown and Michael's vortex model
(a) and (b) are taken from ref [6]

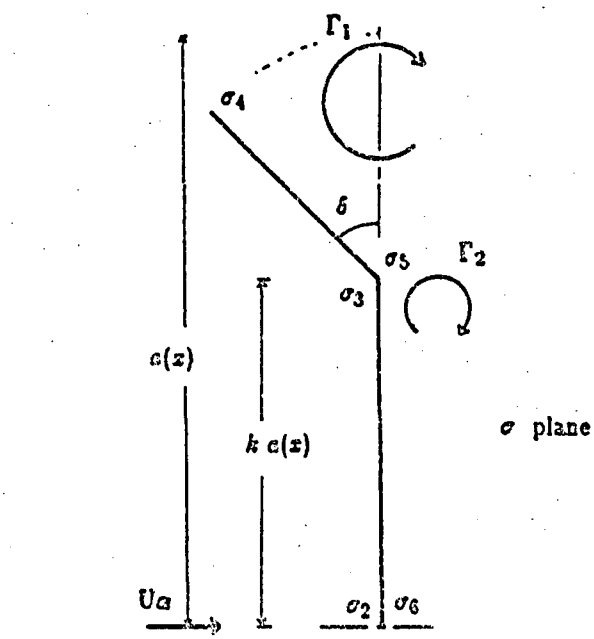

(a) Physical plane

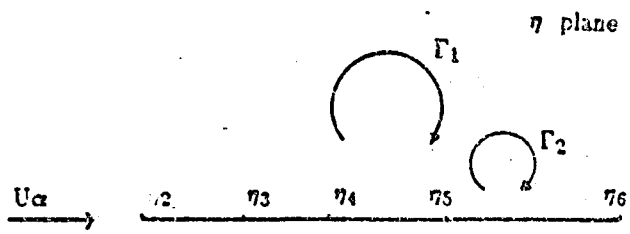

(b) Mapping plane

Fig. 3. Mapping procedure

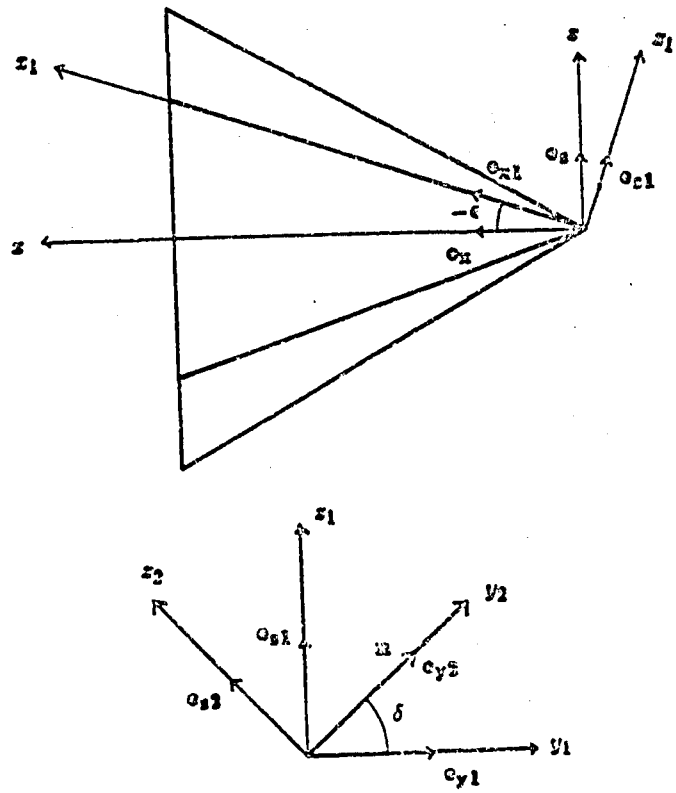

Fig. 4. Coordinate rotation in flap deflection

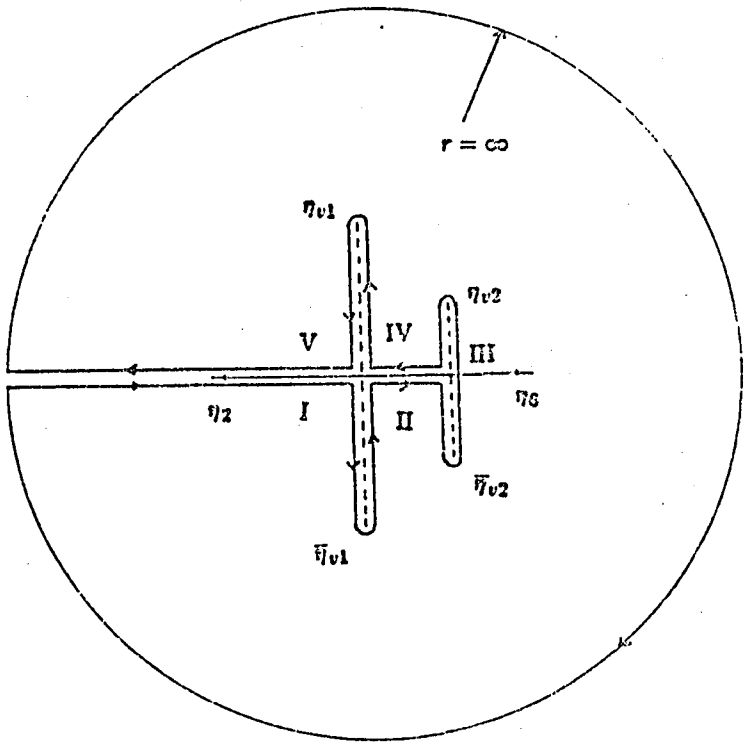

(a) Integration contour for logarithmic terms

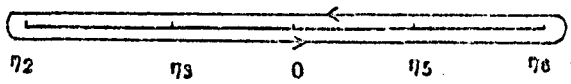

(b) Integration contour for (66)

Fig. 5. Integration contour for normal force

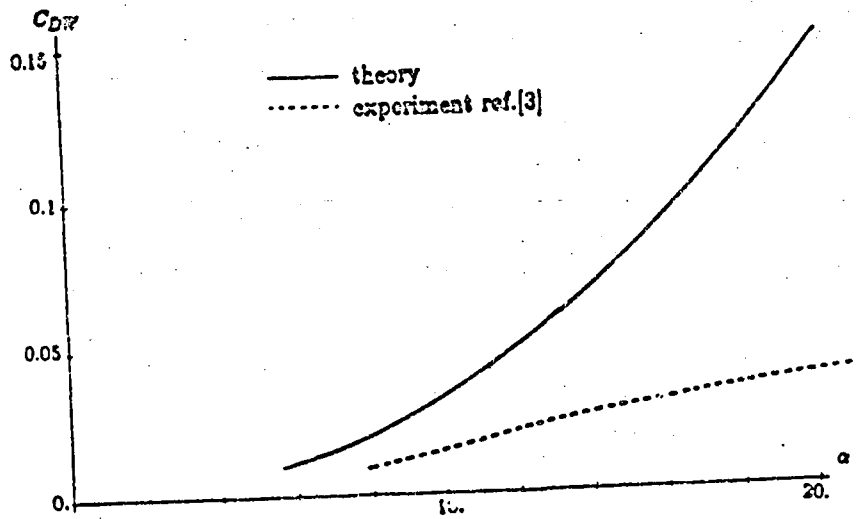

Fig. 6. Drag on main wing

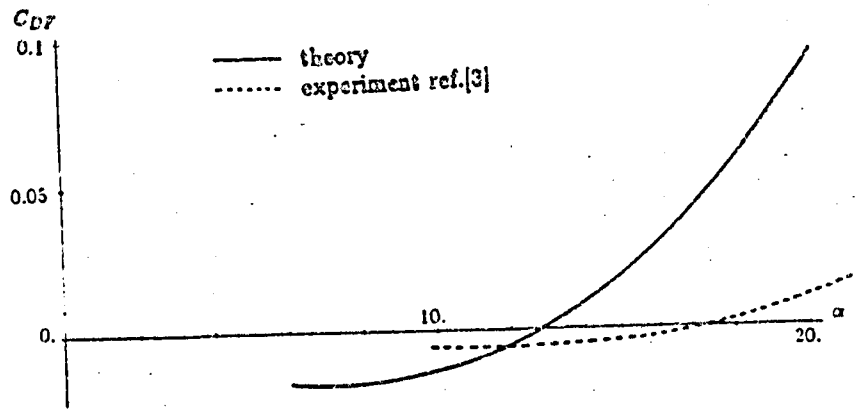

Fig. 7. Drag on flap

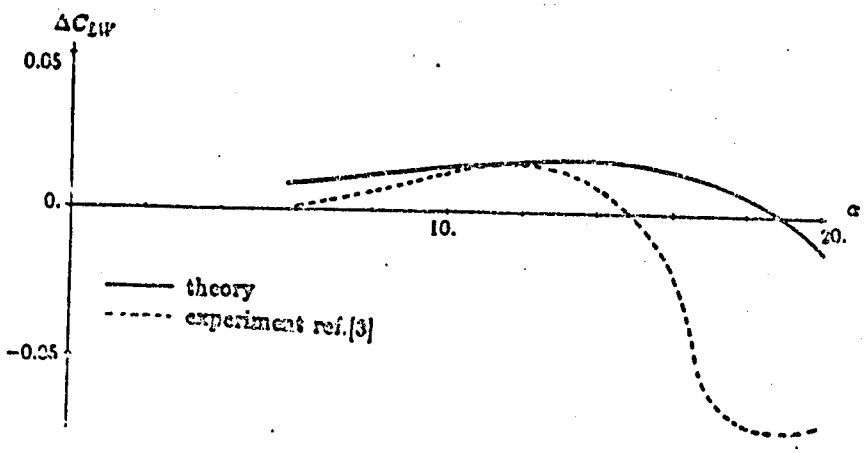

Fig. 8. Lift increment on main wing

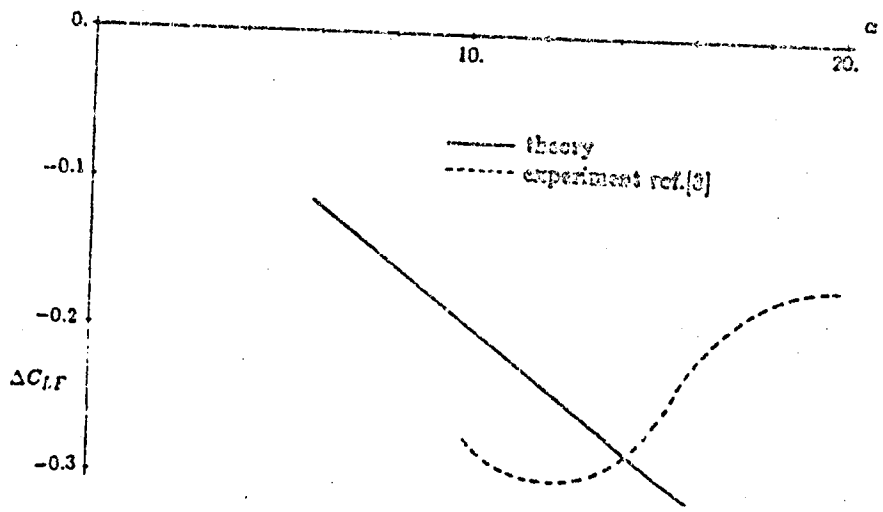

Fig. 9. Lift increment on flap

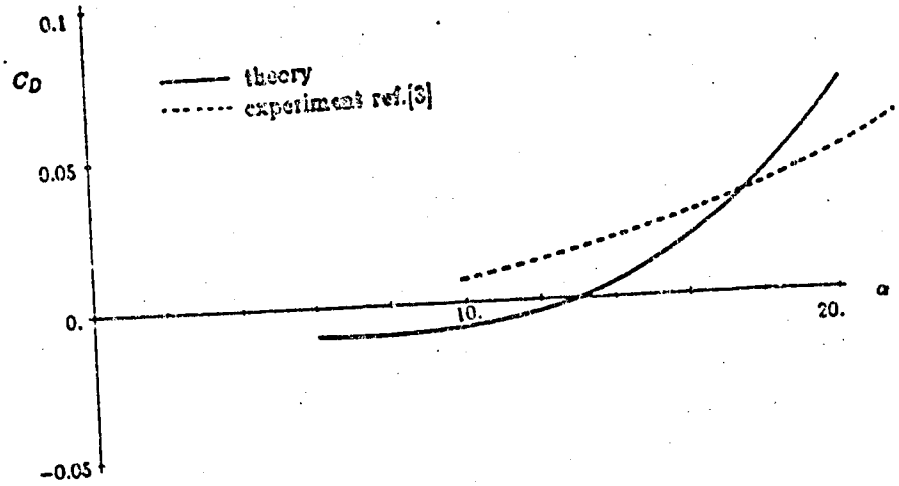

Fig. 10. Total drag

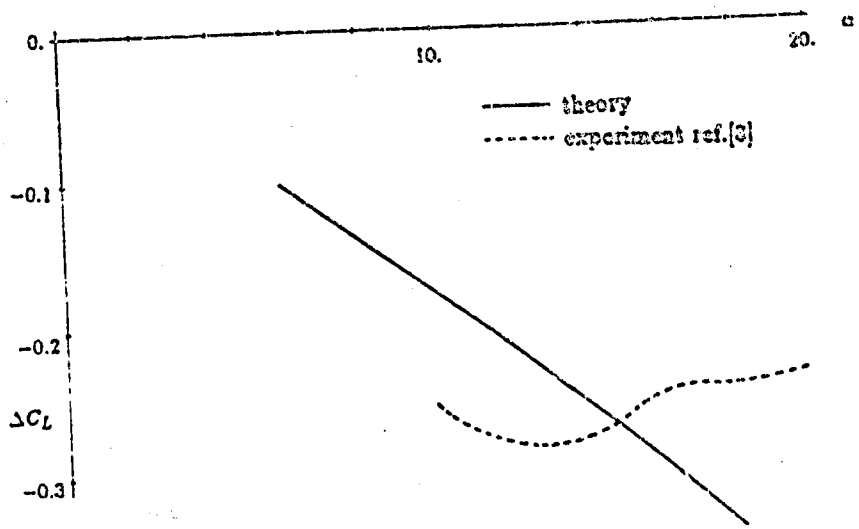

Fig. 11. Total lift increment

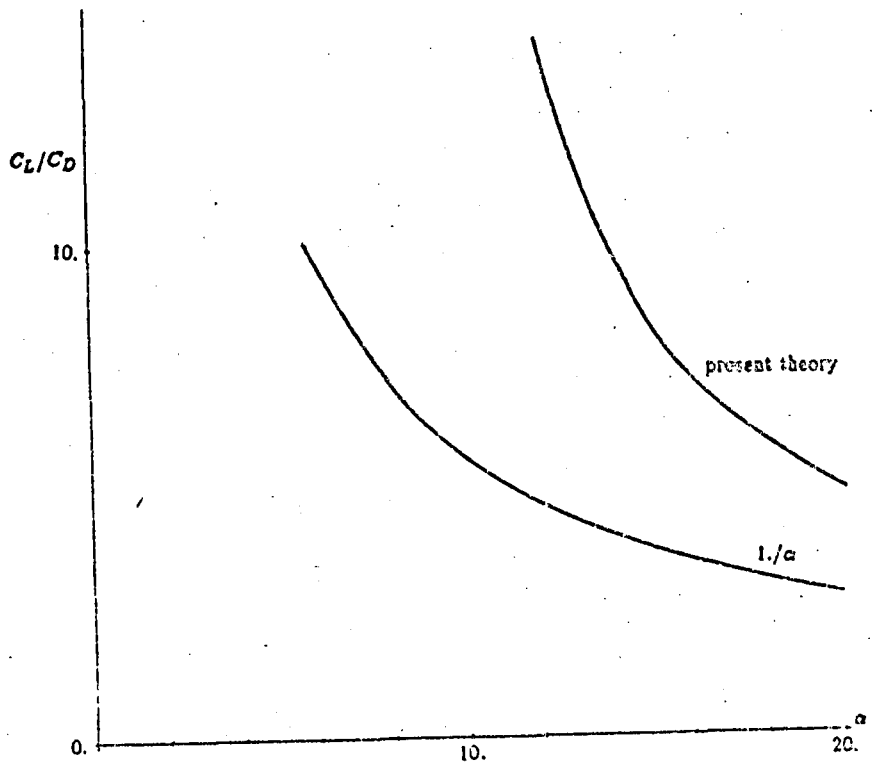

Fig. 12. Lift-to-drag ratio

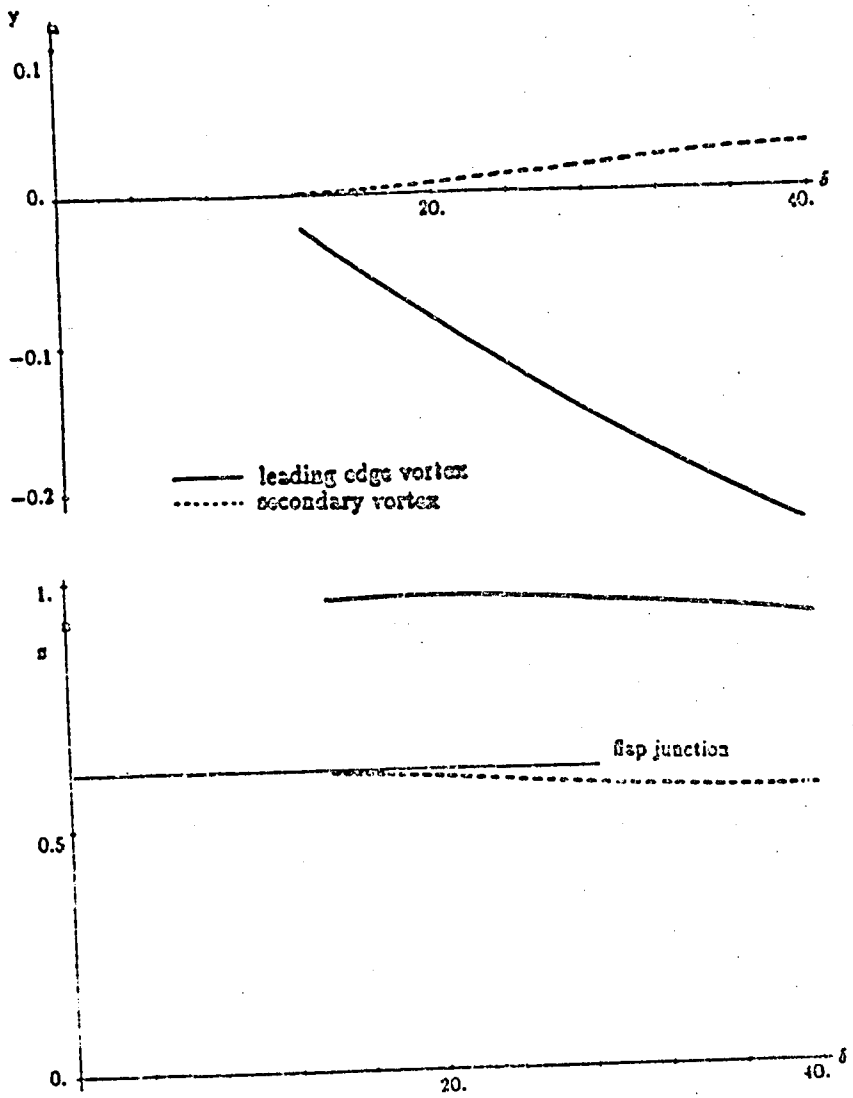

Fig. 13. Vortex position for $\alpha = 10^{o}$

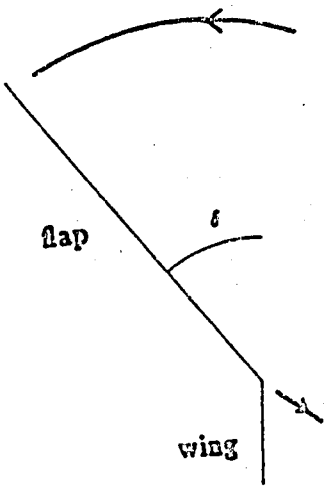

Fig. 14. Vortex loci
⟶ : direction of loci as δ increases

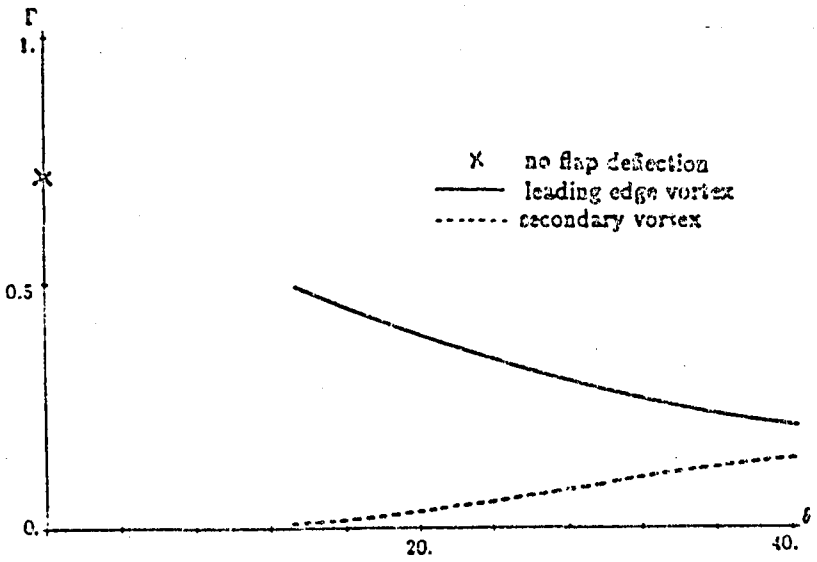

Fig. 15. Vortex strength for $\alpha = 10^{\circ}$

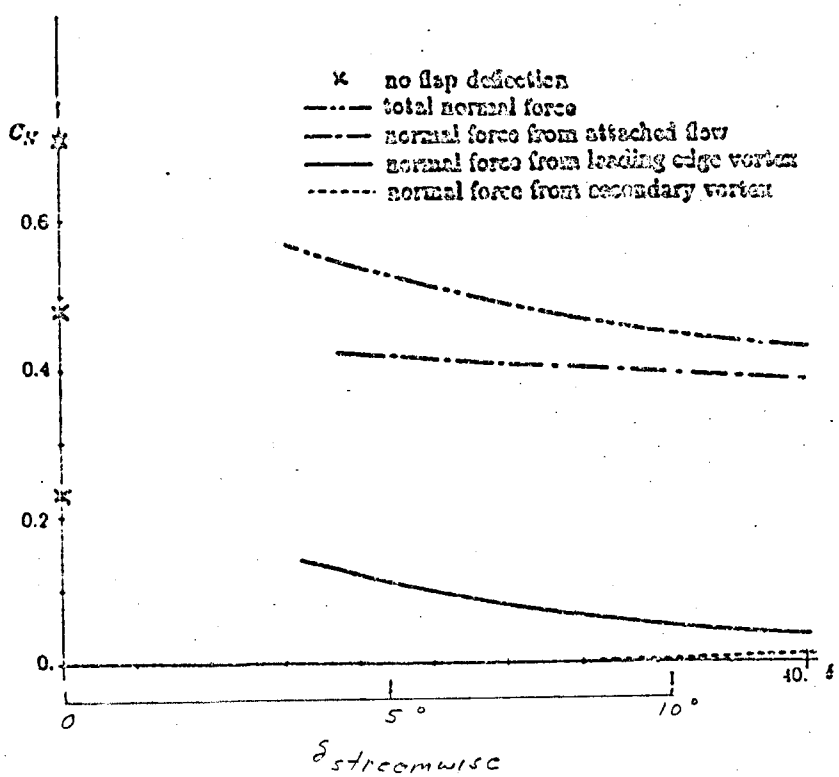

Fig. 16. Normal force components for $\alpha = 10^{o}$

APPENDIX

A 1. Numerical procedure for conformal mapping

A 1.1 Wolfe method

Wolfe's method is just a variation on the secant method for systems of nonlinear equations. This method has the advantage that as the solution becomes closer to the root, the convergence speed is much faster than that of Newton-Raphson methods. For a single equation the secant method is equvalent to solving the following two equations, with two initial guesses

$$p_1 + p_2 = 1 \tag{A1.1a}$$

$$p_1 f(x_n) + p_2 f(x_{n-1}) = 0 \tag{A1.1b}$$

The solution is updated as

$$x_{n+1} = p_1 x_{n-1} + p_2 x_n \tag{A1.1c}$$

For a system of n equations a set of $n+1$ equations must be solved with $n+1$ vectors of initial guesses,

$$\sum_{j=1}^{n+1} p_j = 1 \tag{A1.2a}$$

$$\sum_{j=1}^{n+1} p_j f_i(x_1^j, x_2^j, \cdots, x_n^j) = 0 \quad i = 1, 2, \cdots, n \ . \tag{A1.2b}$$

For the solution update we ignore the vector x^j which gives the maximum residue.

$$x^j|_{k+1^{th}\ step} = \sum_{j=1}^{n+1} p_j x^j|_{k^{th}\ step} \ , \tag{A1.3}$$

where $x^j = (x_1^j, x_2^j, \cdots, x_n^j)$.

This procedure is repeated until the maximum residue becomes smaller than a given value.

A 1.2 Integration at singular points

The integrand of the mapping function is singular at the points $\xi = \eta_2, \eta_3, \eta_5$. To perform the numerical integration, the integrand is expanded to 1st order in Taylor series about those points. For example, at $\xi = \eta_2$

$$\begin{aligned}
&\int_{\eta_2}^{\eta_2+\varepsilon} \frac{\xi}{\sqrt{(\eta_5-\xi)(\xi-\eta_2)}}\left(\frac{\eta_5-\xi}{\eta_3-\xi}\right)^{\delta/\pi} d\xi \\
&= \int_0^{\varepsilon} \frac{\zeta+\eta_2}{\sqrt{\zeta(\eta_5-\zeta-\eta_2)}}\left(\frac{\eta_5-\zeta-\eta_2}{\eta_3-\zeta-\eta_2}\right)^{\delta/\pi} d\zeta \\
&\simeq \frac{\eta_2}{\sqrt{\eta_5-\eta_2}}\left(\frac{\eta_5-\eta_2}{\eta_3-\eta_2}\right)^{\delta/\pi} \int_0^{\varepsilon} \frac{1}{\sqrt{\zeta}}\, d\zeta \\
&= \frac{2\eta_2}{\sqrt{\eta_5-\eta_2}}\left(\frac{\eta_5-\eta_2}{\eta_3-\eta_2}\right)^{\delta/\pi}\sqrt{\varepsilon}
\end{aligned} \tag{A1.4}$$

where $\zeta = \xi - \eta_2$.

Romberg integration is used on the rest of the range.

A 2. Numerical procedure for the vortex positions

A 2.1 Newton - Raphson method for complex functions

Consider the system of real equations

$$\mathbf{f}(\mathbf{x}) = 0 \tag{A.2.1}$$

The general form of the Newton-Raphson method is

$$\mathbf{x}_{n+1} = \mathbf{x}_n - J^{-1}[\mathbf{f}(\mathbf{x}_n)]\ \mathbf{f}(\mathbf{x}_n) \tag{A.2.2}$$

where $J[\mathbf{f}(\mathbf{x}_n)]$ is the Jacobian of $\mathbf{f}(\mathbf{x})$ at $\mathbf{x}_n$.

In the case of a system of complex equations

$$\mathbf{x} = (x_1 + iy_1, x_2 + iy_2, \cdots, x_n + iy_n) \tag{A.2.3}$$

Applying the scheme to the real and imaginary parts of f we get

$$\begin{pmatrix} x_1 \\ y_1 \\ x_2 \\ y_2 \\ \vdots \\ x_n \\ y_n \end{pmatrix}_{n+1} = \begin{pmatrix} x_1 \\ y_1 \\ x_2 \\ y_2 \\ \vdots \\ x_n \\ y_n \end{pmatrix}_n - J^{-1} \begin{pmatrix} \mathrm{Re} f_1 \\ \mathrm{Im} f_1 \\ \mathrm{Re} f_2 \\ \mathrm{Im} f_2 \\ \vdots \\ \mathrm{Re} f_n \\ \mathrm{Im} f_n \end{pmatrix}_n \qquad (A.2.4)$$

with

$$J = \begin{pmatrix} \mathrm{Re}\left(\frac{\partial f_1}{\partial x_1}\right) & \mathrm{Re}\left(\frac{\partial f_1}{\partial y_1}\right) & \cdots & \mathrm{Re}\left(\frac{\partial f_1}{\partial x_n}\right) & \mathrm{Re}\left(\frac{\partial f_1}{\partial y_n}\right) \\ \mathrm{Im}\left(\frac{\partial f_1}{\partial x_1}\right) & \mathrm{Im}\left(\frac{\partial f_1}{\partial y_1}\right) & \cdots & \mathrm{Im}\left(\frac{\partial f_1}{\partial x_n}\right) & \mathrm{Im}\left(\frac{\partial f_1}{\partial y_n}\right) \\ \vdots & \vdots & \ddots & \vdots & \vdots \\ \mathrm{Re}\left(\frac{\partial f_n}{\partial x_1}\right) & \mathrm{Re}\left(\frac{\partial f_n}{\partial y_1}\right) & \cdots & \mathrm{Re}\left(\frac{\partial f_n}{\partial x_n}\right) & \mathrm{Re}\left(\frac{\partial f_n}{\partial y_n}\right) \\ \mathrm{Im}\left(\frac{\partial f_n}{\partial x_1}\right) & \mathrm{Im}\left(\frac{\partial f_n}{\partial y_1}\right) & \cdots & \mathrm{Im}\left(\frac{\partial f_n}{\partial x_n}\right) & \mathrm{Im}\left(\frac{\partial f_n}{\partial y_n}\right) \end{pmatrix}_n \qquad (A.2.5)$$

For the present problem we have two equations for the vortex positions, or a 4×4 matrix. The reason why the Newton - Raphson method is used here is that for Wolfe methods we need one more initial guess than for the Newton - Raphson method, which gives 6×6 matrix. A more important reason is that the Wolfe method needs very accurate initial guesses for good convergence.

A 2.2 Integration path for the mapping function

In using Newton - Raphson method to solve the equations for the vortex positions we need to calculate the corresponding points between the physical plane and the transformed plane by carrying out the transformation

$$\sigma = \int_{\eta_3}^{\eta} \frac{\eta}{\sqrt{(\eta - \eta_2)(\eta - \eta_6)}} \left(\frac{\eta - \eta_5}{\eta - \eta_3}\right)^{\delta/\pi} d\eta \quad . \qquad (A2.6)$$

If we take the integration path as a straight line connecting η_2 with the assumed vortex position, we encounter the following problem: when the vortex position is

very close to the real axis, which is the case when α is small, the integration path almost passes through the singular points η_5 and η_6. To avoid this possible numerical singularity, the integration path is taken in the following way:

$$\eta_2 \rightarrow \eta_2 + i\,2 \rightarrow \text{assumed } \mathrm{Re}\,\eta_v + i\,2 \rightarrow \text{assumed } \eta_v \qquad (A2.7)$$

The maximum imaginary value is taken as 2, which is large enough to calculate the vortex positions.

A 2.3 Velocity at the vortex location

(37) and (38) in chapter 2 contain terms of the form

$$\frac{d}{d\sigma}\Big[log(\eta-\eta_{vi})-log(\sigma-\sigma_{vi})\Big]_{\sigma\rightarrow\sigma_{vi}} , \qquad (A2.8a)$$

which can be written as

$$\frac{d}{d\eta}\Big[log(\eta-\eta_{vi})-log(\sigma-\sigma_{vi})\Big]_{\eta\rightarrow\eta_{vi}}\frac{d\eta}{d\sigma}\Big|_{\sigma_{vi}} \qquad (A2.8b)$$

In terms of finite differences this quantity can be approximated by

$$\begin{aligned}&\left[\left(log\frac{\eta_{vi}+\Delta\eta_{vi}-\eta_{vi}}{\sigma(\eta_{vi}+\Delta\eta_{vi})-\sigma_{vi}}-log\frac{\eta_{vi}-\Delta\eta_{vi}-\eta_{vi}}{\sigma(\eta_{vi}-\Delta\eta_{vi})-\sigma_{vi}}\right)\Big/\left(2\Delta\eta_{vi}\right)\right]\frac{d\eta}{d\sigma}\Big|_{\eta_{vi}}\\ &=\left[\left(log\frac{\sigma_{vi}-\sigma(\eta_{vi}-\Delta\eta_{vi})}{\sigma(\eta_{vi}+\Delta\eta_{vi})-\sigma_{vi}}\right)\Big/\left(2\Delta\sigma_{vi}\right)\right]\frac{d\eta}{d\sigma}\Big|_{\eta_{vi}}\end{aligned} \qquad (A2.9)$$

This is done in the transformed plane to avoid inverting (A 2.6).

A 3. Derivation of the axial velocity component

In 2.4 we derived the axial velocity component under conical flow assumptions

$$u = U+\frac{1}{x}\left(\Phi-y\frac{\partial\Phi}{\partial y}-z\frac{\partial\Phi}{\partial z}\right) \qquad (A3.1a)$$

$$= U+\frac{\epsilon}{k}\mathrm{Re}\left[U\alpha\eta+\frac{i\Gamma_1}{2\pi}log\left(\frac{\eta-\eta_{v1}}{\eta-\bar{\eta}_{v1}}\right)-\frac{i\Gamma_2}{2\pi}log\left(\frac{\eta-\eta_{v2}}{\eta-\bar{\eta}_{v2}}\right)-yv-zw\right] \qquad (A3.1b)$$

Here we have logarithmic branch points at η_{v1}, η_{v2}, $\bar{\eta}_{v1}$, $\bar{\eta}_{v2}$. To numerically evaluate functions across branch cuts care must be exercised since computers usually give the argument of a complex variable between $-\pi$ and π while the value of interest here is between 0 and 2π. As an example we consider two branch points at η_{v1} and $\bar{\eta}_{v1}$, as shown in Fig. 5a

$$log(\eta-\eta_{v1}) = \begin{cases} log(\eta-\eta_{v1})|_p = log(\eta-\eta_{v1})|_c + i\,2\pi & \text{in I,II,III,IV} \\ log(\eta-\eta_{v1})|_p + i\,2\pi = log(\eta-\eta_{v1})|_c + i\,4\pi & \text{in V} \end{cases} \tag{A3.2a}$$

$$log(\eta-\bar{\eta}_{v1}) = \begin{cases} log(\eta-\bar{\eta}_{v1})|_p = log(\eta-\bar{\eta}_{v1})|_c + i\,2\pi & \text{in I} \\ log(\eta-\bar{\eta}_{v1})|_p + i\,2\pi = log(\eta-\bar{\eta}_{v1})|_c + i\,4\pi & \text{in II,III,IV,V} \end{cases} \tag{A3.2b}$$

where the subscript p means the principal value and c means the value calculated from the computer. Actually the values are calculated only in region IV,V and half of III due to the symmetry of the flow.

A 4. Fortran program for the Schwarz-Christoffel transformation

```
      IMPLICIT REAL*8(A-H,O-Z)
      DIMENSION SS(10,10),WORK(10),OA(10,10),Z(10),IPVT(10),XF(10)
     *         ,FNRM(10),X(10,10),XZ(10),B(10),XX(10),VX(10),SX(10)
      DATA IMAX,JMAX/4,5/
      DATA PI/3.141592654/
      DATA ERR,EPS/1.D-8,1.D-2/
      DATA XRTO / .6153846154 /
C     WRITE(6,700) XRTO
C700  FORMAT(5X,' FLAP ANGLE  = ',D15.6)
      DO 1 J=1,JMAX
1     READ(35,*)(X(I,J),I=1,IMAX)
      WRITE(30,121)
111   READ(5,*) DLTAD
      DLTA=DLTAD*PI/180.
      N=0
5     DO 2 J=1,JMAX
      DO 3 I=1,IMAX
3     VX(I)=X(I,J)
      CALL MATEL(VX,IMAX,JMAX,PI,XRTO,DLTA,ERR,EPS,SX)
      DO 4 I=1,IMAX
4     SS(I,J)=SX(I)
      SS(JMAX,J)=1.
2     CONTINUE
      DO 6 I=1,IMAX
6     B(I)=0.
      B(JMAX)=1
      CALL DECOMP(10,JMAX,SS,COND,IPVT,WORK,OA,Z,ZNORM)
      CALL SOLVE(10,JMAX,SS,B,IPVT,XZ)
      DO 7 I=1,IMAX
      XX(I)=0.
      DO 7 J=1,JMAX
7     XX(I)=XX(I)+X(I,J)*XZ(J)
      CALL NORM(OA,IMAX,JMAX,FMX,FNRM,XLOG,JC)
      IF(XLOG.LT.-10.) GO TO 8
      IF(N.GT.50) GO TO 9
      DO 10 I=1,IMAX
10    X(I,JC)=XX(I)
      N=N+1
      WRITE(6,500)N,(X(I,JC),I=1,IMAX)
      X(1,JC)=-DABS(X(1,JC))
      X(2,JC)=-DABS(X(2,JC))
      X(3,JC)=DABS(X(3,JC))
      X(4,JC)=DABS(X(4,JC))
      IF(X(2,JC).LT.X(3,JC)) GO TO 300
      CXX=X(2,JC)
      X(2,JC)=X(3,JC)
```

```
      X(3,JC)=CXX
      GO TO 300
300   IF(X(3,JC).LT.X(4,JC)) GO TO 400
      CYY=X(4,JC)
      X(4,JC)=X(3,JC)
      X(3,JC)=CYY
      GO TO 400
400   GO TO 5
9     WRITE(6,100)
      GO TO 11
8     WRITE(6,500)N,(XX(I),I=1,IMAX)
      GO TO 11
11    WRITE(30,202)DLTAD,(XX(I),I=1,IMAX)
      IF(XRTO.GT.2.) GO TO 130
      GO TO 111
130   STOP
121   FORMAT(3X,'DLTA',9X,'A2',14X,'A3',14X,'A5',14X,'A6',1X/)
100   FORMAT(1X,'MORE THAN 50 ITERATION')
202   FORMAT(1X,F8.5,4(1X,D15.6))
500   FORMAT(1X,I2,4(1X,D15.6))
      END

      SUBROUTINE MATEL(X,IMAX,JMAX,PI,XRTO,DLTA,ERR,EPS,Y)
      IMPLICIT REAL*8 (A-H,O-Z)
      DIMENSION X(10),Y(10)
      A2=X(1)
      A3=X(2)
      A5=X(3)
      A6=X(4)
      A2P=A2+EPS
      A3M=A3-EPS
      A3P=A3+EPS
      A6M=A6-EPS
      CALL ROMBRG(1,A2,A3,A5,A6,A2P,A3M,ERR,DLTA,PI,XINT1)
      CALL ROMBRG(2,A2,A3,A5,A6,A3P,0.,ERR,DLTA,PI,XINT2)
      CALL ROMBRG(2,A2,A3,A5,A6,0.,A5,ERR,DLTA,PI,XINT3)
      CALL ROMBRG(3,A2,A3,A5,A6,A5,A6M,ERR,DLTA,PI,XINT4)
      Y(1)=XRTO+XINT1+2.*A2*((A5-A2)/(A3-A2))**(DLTA/PI)
     *                *DSQRT(EPS/(A6-A2))+A3*(A5-A3)**(DLTA/PI)
     *                *EPS**(1.-DLTA/PI)/((1.-DLTA/PI)*DSQRT(
     *                (A6-A3)*(A3-A2)))
      Y(2)=1.-XRTO+
     *                   XINT2+A3*(A5-A3)**(DLTA/PI)*EPS**(1.-DLTA/PI)/
     *                   ((1.-DLTA/PI)*DSQRT((A6-A3)*(A3-A2)))
      Y(3)=1.-XRTO-XINT3
      Y(4)=XRTO-XINT4-
     *                2.*A6*((A6-A5)/(A6-A3))**(DLTA/PI)*DSQRT(EPS/(A6-A2))
      RETURN
      END
```

```
      SUBROUTINE NORM(X,IM,JM,XMAX,XNRM,XLOG,N)
      IMPLICIT REAL*8(A-H,O-Z)
      DIMENSION X(10,10),XNRM(10)
      XMAX=0.
      N=1
      DO 2 J=1,JM
      XNRM(J)=0.
      DO 1 I=1,IM
1     XNRM(J)=XNRM(J)+X(I,J)**2
      IF(XMAX.GT.XNRM(J)) GO TO 2
      XMAX=XNRM(J)
      N=J
2     CONTINUE
      XLOG=DLOG(XMAX)
      RETURN
      END

      SUBROUTINE DECOMP(NDIM,N,A,COND,IPVT,WORK,CA,Z,ZNORM)
      IMPLICIT REAL*8(A-H,O-Z)
      DIMENSION A(NDIM,N),WORK(N),CA(NDIM,N),Z(N),IPVT(N)
      INTEGER NM1,I,J,K,KP1,KB,KM1,M
      DO 1 I=1,N
      DO 1 J=1,N
      CA(I,J)=A(I,J)
1     CONTINUE
      IPVT(N)=1
      IF(N.EQ.1) GO TO 80
      NM1=N-1
      ANORM=0.
      DO 10 J=1,N
      T=0.
      DO 5 I=1,N
      T=T+ABS(A(I,J))
5     CONTINUE
      IF(T.GT.ANORM) ANORM=T
10    CONTINUE
      DO 35 K=1,NM1
      KP1=K+1
      M=K
      DO 15 I=KP1,N
      IF(ABS(A(I,K)).GT.ABS(A(M,K))) M=I
15    CONTINUE
      IPVT(K)=M
      IF(M.NE.K) IPVT(N)=-IPVT(N)
      T=A(M,K)
      A(M,K)=A(K,K)
      A(K,K)=T
      IF(T.EQ.0.) GO TO 35
      DO 20 I=KP1,N
      A(I,K)=-A(I,K)/T
```

```
   20   CONTINUE
        DO 30 J=KP1,N
        T=A(M,J)
        A(M,J)=A(K,J)
        A(K,J)=T
        IF(T.EQ.0.) GO TO 30
        DO 25 I=KP1,N
        A(I,J)=A(I,J)+A(I,K)*T
   25   CONTINUE
   30   CONTINUE
   35   CONTINUE
        DO 50 K=1,N
        T=0.
        IF(K.EQ.1) GO TO 45
        KM1=K-1
        DO 40 I=1,KM1
        T=T+A(I,K)*WORK(I)
   40   CONTINUE
   45   EK=1.
        IF(T.LT.0.) EK=-1.
        IF(A(K,K).EQ.0.) GO TO 90
        WORK(K)=-(EK+T)/A(K,K)
   50   CONTINUE
        DO 60 KB=1,NM1
        K=N-KB
        T=0.
        KP1=K+1
        DO 55 I=KP1,N
        T=T+A(I,K)*WORK(K)
   55   CONTINUE
        WORK(K)=T
        M=IPVT(K)
        IF(M.EQ.K) GO TO 60
        T=WORK(M)
        WORK(M)=WORK(K)
        WORK(K)=T
   60   CONTINUE
        YNORM=0.
        DO 65 I=1,N
        YNORM=YNORM+ABS(WORK(I))
   65   CONTINUE
        CALL SOLVE(NDIM,N,A,WORK,IPVT,Z)
        ZNORM=0.
        DO 70 I=1,N
        ZNORM=ZNORM+ABS(Z(I))
   70   CONTINUE
        COND=ANORM*ZNORM/YNORM
        IF(COND.LT.1.) COND=1.
        RETURN
```

```
80      COND=1.
        IF(A(1,1).NE.0.) RETURN
90      COND=1.E+32
        RETURN
        END



        SUBROUTINE SOLVE(NDIM,N,A,B,IPVT,X)
         IMPLICIT REAL*8(A-H,O-Z)
         DIMENSION IPVT(N),A(NDIM,N),B(N),X(N)
        DO 1 I=1,N
        X(I)=B(I)
1       CONTINUE
        IF(N.EQ.1) GO TO 50
        NM1=N-1
        DO 20 K=1,NM1
        KP1=K+1
        M=IPVT(K)
        T=X(M)
        X(M)=X(K)
        X(K)=T
        DO 10 I=KP1,N
        X(I)=X(I)+A(I,K)*T
10      CONTINUE
20      CONTINUE
        DO 40 KB=1,NM1
        KM1=N-KB
        K=KM1+1
        X(K)=X(K)/A(K,K)
        T=-X(K)
        DO 30 I=1,KM1
        X(I)=X(I)+A(I,K)*T
30      CONTINUE
40      CONTINUE
50      X(1)=X(1)/A(1,1)
        RETURN
        END


         SUBROUTINE ROMBERG(N,A2,A3,A5,A6,A,B,ERR,DLTA,PI,RES)
         IMPLICIT REAL*8(A-H,O-Z)
         DIMENSION Z(10,10)
         I=1
         DEL=B-A
         IF(N-2)30,40,50
30       Z(1,1)=.5*DEL*(FUN1(A,A2,A3,A5,A6,DLTA,PI)
     *          +FUN1(B,A2,A3,A5,A6,DLTA,PI))
         GO TO 10
```

```
40      Z(1,1)=.5*DEL*(FUN2(A,A2,A3,A5,A6,DLTA,PI)
     *          +FUN2(B,A2,A3,A5,A6,DLTA,PI))
        GO TO 10
50      Z(1,1)=.5*DEL*(FUN3(A,A2,A3,A5,A6,DLTA,PI)
     *          +FUN3(B,A2,A3,A5,A6,DLTA,PI))
        GO TO 10
10      J=IFIX(2.**(I-1))
        DEL=DEL/2.
        I=I+1
        Z(I,1)=.5*Z(I-1,1)
        DO 1 K=1,J
        X=A+(2.*FLOAT(K)-1.)*DEL
        IF(N-2) 60,70,80
60      Z(I,1)=Z(I,1)+DEL*FUN1(X,A2,A3,A5,A6,DLTA,PI)
        GO TO 1
70      Z(I,1)=Z(I,1)+DEL*FUN2(X,A2,A3,A5,A6,DLTA,PI)
        GO TO 1
80      Z(I,1)=Z(I,1)+DEL*FUN3(X,A2,A3,A5,A6,DLTA,PI)
        GO TO 1
1       CONTINUE
        DO 2 K=2,I
        Z(I,K)=(4.**(K-1)*Z(I,K-1)-Z(I-1,K-1))/(4.**(K-1)-1.)
2       CONTINUE
        DIFF=DABS(Z(I,I)-Z(I,I-1))
        IF(DIFF.LT.ERR) GO TO 20
        GO TO 10
20      RES=Z(I,I)
        RETURN
        END


        FUNCTION FUN1(X,A2,A3,A5,A6,DLTA,PI)
        IMPLICIT REAL*8(A-H,O-Z)
        FUN1=X*((A5-X)/(A3-X))**(DLTA/PI)/DSQRT((A6-X)*(X-A2))
        RETURN
        END


        FUNCTION FUN2(X,A2,A3,A5,A6,DLTA,PI)
        IMPLICIT REAL*8(A-H,O-Z)
        FUN2=X*((A5-X)/(X-A3))**(DLTA/PI)/DSQRT((A6-X)*(X-A2))
        RETURN
        END


        FUNCTION FUN3(X,A2,A3,A5,A6,DLTA,PI)
        IMPLICIT REAL*8(A-H,O-Z)
        FUN3=X*((X-A5)/(X-A3))**(DLTA/PI)/DSQRT((A6-X)*(X-A2))
        RETURN
        END
```

A 6. Fortran program for the aerodynamic forces

```
C*****************************************************************************
C
C       DELTA WING WITH FLAP PROBLEM
C         WITH ONLY ONE VORTEX FROM LEADING EDGE
C               USING NEWTON-RAPHSON METHODS
C                     WITH DIFFERENT INTEGRATING PATH
C
C*****************************************************************************

      IMPLICIT INTEGER*4(I-N)
      COMPLEX*16 XI,X,Z,W
      REAL*8     ERR,PI,ALP,APX,XK1,XK2,DLT,A2,A3,A5,A6,GAM,ALPD
     *           CL3,CLW,CDW,CLF,CDF,CLT,CDT,CLL,TCL,TCD,RTOR,RTO
      DIMENSION Z(10),W(10),GAM(10)
      COMMON /DATA1/ IMAX,JMAX
      COMMON /DATA2/ XI,ERR,PI
      COMMON /DATA3/ ALP,APX
      COMMON /DATA4/ X(10)
      COMMON /DATA5/ XK1,XK2,DLT
      COMMON /DATA6/ A2,A3,A5,A6

      DO 100 I=1,10
      CALL DATA(ALPD)

      CALL NEWTON(Z,W)

      CALL VORTEX(W,GAM)

C     CALL PRESSURE(W,GAM)

      CALL LIFT(GAM,W,CL3)

C     CALL LIFT1(GAM,W,CLW,CDW,CLF,CDF,CLT,CDT,CLL,
C    *           TCL,TCD,RTOR,RTO)
C     WRITE(6,300)ALPD,CL3,CLW,CDW,CLF,CDF,CLT,CDT,CLL
C    *           ,TCL,TCD,RTOR,RTO

100   CONTINUE
300   FORMAT(1X,F5.2,1X,D11.4/5X,6(1X,D11.4)/5X,5(1X,D11.4))
200   FORMAT(2X,'DLT',5X,'VORTEX POSITION',9X,'GAM',9X,
     *       'CLL',9X,'CLV',9X,'CLT'/)
      STOP
      END
```

```
      SUBROUTINE DATA(ALPD)

C       INPUT OF DATA USED IN THE WHOLE PROGRAM

C       IMAX   : RNAK OF MATRIX i.e. THE NUMBER OF UNKNOWNS
C       JMAX   : 5 FOR NEWTON-RAPHSON METHODS (I-1,J),(I+1,J),(I,J-1)
C                                              ,(I,J+1),(I,J)
C
C       XI     : SQRT(-1)
C       ERR    : CONVERGENCE OF ROMBERG INTEGRATION
C       PI     : 3.14.....
C       ALP    : ANGLE OF ATTACK
C       APX    : HALF OF APEX ANGLE OF MAIN DELTA WING
C       X(I)   : INITIAL GUESS
C       XK     : RATIO OF MAIN DELTA WING TO TOTAL SPAN LENGTH (=1)
C       DLT    : FALP DEFLECTION ANGLE
C       A2,A3,A5,A6 : COEFF. OF SCHWARTZ-CHRISTOFFEL TRANSFORMATION
C
      IMPLICIT INTEGER*4(I-N)
      COMPLEX*16 XI,X
      REAL*8     ERR,PI,ALP,APX,XK1,XK2,DLT,A2,A3,A5,A6,ALPD,DLTD
      COMMON /DATA1/ IMAX,JMAX
      COMMON /DATA2/ XI,ERR,PI
      COMMON /DATA3/ ALP,APX
      COMMON /DATA4/ X(10)
      COMMON /DATA5/ XK1,XK2,DLT
      COMMON /DATA6/ A2,A3,A5,A6
      DATA ERR,PI / 1.D-6, 3.141592654 /
      DATA XI / (0.,1.) /
      DATA IMAX,JMAX / 1, 5 /
      DATA ALP,APX / .17453278   , .2685121925 /
      DATA XK1,XK2 / .6153846154, .8846153846 /
C     DATA A2,A3,A5,A6 / -0.636893, -0.515968,
C    *                    0.978499,  1.3006   /
      WRITE(6,1)
      READ(5,*)DLTD
C     READ(5,*)ALPD
      DLT=DLTD*PI/180.
      WRITE(6,2)
      READ(5,*)A2,A3,A5,A6
      WRITE(34,100)ALP,APX,XK1,XK2,DLT,A2,A3,A5,A6
      WRITE(6,600)
      READ(5,*)(X(I),I=1,IMAX)
1     FORMAT(1X,'DLT')
2     FORMAT(1X,'TRANS. COEFF.')
100   FORMAT(/5X,'1. GIVEN DATA '/
     *        8X,'ANGLE OF ATTACK = ',D11.4/
     *        8X,'APEX ANGLE      = ',D11.4/
     *        8X,'FLPA      RATIO = ',D11.4/
     *        8X,'TAP       RATIO = ',D11.4/
     *        8X,'FLAP ANGLE      = ',D11.4/
     *        8X,'TRAN. COEFF. :',4(2X,D11.4)/)
```

```
600   FORMAT(1X,' INITIAL GUESS')
      RETURN
      END



      SUBROUTINE NEWTON(VZ,VW)

C       CALCULATION OF VORTEX POSITION

      IMPLICIT INTEGER*4(I-N)
      COMPLEX*16 XI,X,W,WN,Z,ZM,DER,DERM,VZ,VW
      REAL*8     ERR,PI,ALP,APX,XK1,XK2,DLT,A2,A3,A5,A6,SS,B,XZ,OA
      DIMENSION W(10,10),
     *          WN(10),Z(10),DER(10),ZM(10,10),DERM(10,10),
     *          SS(10,10),B(10),
     *          IPVT(10),OA(10,10),XZ(10),
     *          VZ(10),VW(10)
      COMMON /DATA1/ IMAX,JMAX
      COMMON /DATA2/ XI,ERR,PI
      COMMON /DATA3/ ALP,APX
      COMMON /DATA4/ X(10)
      COMMON /DATA5/ XK1,XK2,DLT
      COMMON /DATA6/ A2,A3,A5,A6
      N=0
100   CALL NEWPNT(X,W)
      DO 4 I=1,IMAX
        DO 5 J=1,JMAX
5       WN(J)=W(I,J)
        CALL ZCALC(WN,Z,DER)
        DO 6 J=1,JMAX
          ZM(I,J)=Z(J)
6       DERM(I,J)=DER(J)
4     CONTINUE
      CALL MATEL(W,ZM,DERM,SS,B)
      CALL NORM(B,XLOG)
      IF(N.GT.50) GO  TO 11
      IF(XLOG.LT.-7.) GO TO 11
      CALL DECOMP(SS,IPVT,OA)
      CALL SOLVE(SS,B,IPVT,XZ)
      CALL NEXPNT(X,XZ)
      WRITE(6,113)N,XLOG,(ZM(I,5),I=1,IMAX),(W(I,5),I=1,IMAX)
      N=N+1
      GO TO 100
11    WRITE(6,113)N,XLOG,(ZM(I,5),I=1,IMAX),(W(I,5),I=1,IMAX)
      DO 12 I=1,IMAX
        VZ(I)=ZM(I,5)
12    VW(I)=W(I,5)
      WRITE(34,200) VZ(1),VW(1)
```

```
113   FORMAT(1X,I2,5X,' MAXNRM = ',D15.6/
     *       5X,'Z=',2D15.6/
     *       5X,'W=',2D15.6)
200   FORMAT(/5X,'2. VORTEX POSITION. '/
     *        8X,'VORTEX POSITION IN Z-PLANE : ',2D11.4/
     *        8X,'VORTEX POSITION IN W-PLANE : ',2D11.4/)
      RETURN
      END



      SUBROUTINE NEWPNT(XN,YN)
      IMPLICIT INTEGER*4(I-N)
      COMPLEX*16 XN,YN,XI
      REAL*8     ERR,PI,XRE,XIM
      DIMENSION XN(10),YN(10,10)
      COMMON /DATA1/ IMAX,JMAX
      COMMON /DATA2/ XI,ERR,PI

      DO 1 I=1,IMAX
        XRE=DREAL(XN(I))/100.
        XIM=DIMAG(XN(I))/100.
        YN(I,1)=XN(I)-XRE
        YN(I,2)=XN(I)+XRE
        YN(I,3)=XN(I)-XI*XIM
        YN(I,4)=XN(I)+XI*XIM
1     YN(I,5)=XN(I)
      RETURN
      END



      SUBROUTINE MATEL(X,Z,DER,S,BB)
      IMPLICIT INTEGER*4(I-N)
      COMPLEX*16 X,Z,DER,XI,A,B,C,FUN2
      REAL*8     S,BB,ERR,PI,ALP,APX,XK1,XK2,DLT,A2,A3,A5,A6
      DIMENSION X(10,10),Z(10,10),DER(10,10),S(10,10),BB(10)
      COMMON /DATA2/ XI,ERR,PI
      COMMON /DATA3/ ALP,APX
      COMMON /DATA5/ XK1,XK2,DLT
      COMMON /DATA6/ A2,A3,A5,A6
      A=(FUN2(X(1,2),Z(1,2),DER(1,2))-
     *   FUN2(X(1,1),Z(1,1),DER(1,1)))/
     *  (X(1,2)-X(1,1))
      B=(FUN2(X(1,4),Z(1,4),DER(1,4))-
     *   FUN2(X(1,3),Z(1,3),DER(1,3)))/
     *  ((X(1,4)-X(1,3))*(-XI))
      C=FUN2(X(1,5),Z(1,5),DER(1,5))
```

```
      S(1,1)=DREAL(A)
      S(1,2)=DREAL(B)
      S(2,1)=DIMAG(A)
      S(2,2)=DIMAG(B)
      BB(1)=-DREAL(O)
      BB(2)=-DIMAG(O)
      RETURN
      END


      SUBROUTINE NORM(X,XLOG)
      IMPLICIT INTEGER*4(I-N)
      IMPLICIT REAL*8 (A-H,O-Z)
      DIMENSION X(10)
      COMMON /DATA1/ IMAX,JMAX
      IM=IMAX*2
      XNORM=0.
      DO 2 J=1,IM
    2 XNORM=XNORM+(DABS(X(J)))**2
      XLOG=DLOG10(XNORM)
      RETURN
      END



      SUBROUTINE NEXPNT(X,Y)
      IMPLICIT INTEGER*4(I-N)
      COMPLEX*16 X,XI
      REAL*8     Y,ERR,PI
      DIMENSION X(10),Y(10)
      COMMON /DATA2/ XI,ERR,PI
      X(1)=X(1)+Y(1)+XI*Y(2)
      X(1)=DREAL(X(1))+XI*(DABS(DIMAG(X(1))))
      RETURN
      END


      SUBROUTINE ROMBRG(IS,A,B,RES)
      IMPLICIT INTEGER*4(I-N)
      COMPLEX*16 A,B,RES,XI,Z,DEL,FUN1,X,DIFF,FUN5
      REAL*8     ERR,PI
      DIMENSION Z(10,10)
      COMMON /DATA2/ XI,ERR,PI
      I=1
      DEL=B-A
      IF(IS.EQ.1) GO TO 111
      Z(1,1)=.5*DEL*(FUN5(A)+FUN5(B))
      GO TO 10
  111 Z(1,1)=.5*DEL*(FUN1(A)+FUN1(B))
   10 J=IFIX(2.**(I-1))
```

```
      DEL=DEL/2.
      I=I+1
      Z(I,1)=.5*Z(I-1,1)
      DO 1 K=1,J
        X=A+(2.*FLOAT(K)-1.)*DEL
        IF(IS.EQ.1) GO TO 3
        Z(I,1)=Z(I,1)+DEL*FUN5(X)
        GO TO 1
3       Z(I,1)=Z(I,1)+DEL*FUN1(X)
1     CONTINUE
      DO 2 K=2,I
        Z(I,K)=(4.**(K-1)*Z(I,K-1)-Z(I-1,K-1))/(4.**(K-1)-1.)
2     CONTINUE
      DIFF=Z(I,I)-Z(I,I-1)
      IF(CDABS(DIFF).LT.ERR) GO TO 20
      GO TO 10
20    RES=Z(I,I)
      RETURN
      END


      FUNCTION FUN1(X)
      IMPLICIT INTEGER*4(I-N)
      COMPLEX*16 X,XI,FUN1
      REAL*8     ERR,PI,XK1,XK2,DLT,A2,A3,A5,A6
      COMMON /DATA2/ XI,ERR,PI
      COMMON /DATA5/ XK1,XK2,DLT
      COMMON /DATA6/ A2,A3,A5,A6
      FUN1=X*(X-A5)**(DLT/PI)/(CDSQRT(X-A2)*CDSQRT(X-A6)
     *                         *(X-A3)**(DLT/PI))
      RETURN
      END



      SUBROUTINE ZCALC(V,Z,DER)
      IMPLICIT INTEGER*4(I-N)
      COMPLEX*16 V,Z,DER,XI,EPS,SING,B,DB,BP,BM,A2P,RB,RBP,
     *           RBM,P2,P3P,P3M,XINT,XINT1,XINT2,XINT1P,XINT2P,
     *           XINT1M,XINT2M,ZM,ZP,C1,C2,C3
      REAL*8     ERR,PI,XK1,XK2,DLT,A2,A3,A5,A6
      DIMENSION V(10),Z(10),DER(10)
      COMMON /DATA1/ IMAX,JMAX
      COMMON /DATA2/ XI,ERR,PI
      COMMON /DATA5/ XK1,XK2,DLT
      COMMON /DATA6/ A2,A3,A5,A6
      EPS=0.01*XI
      C1=A2-A5
      C2=A2-A6
      C3=A2-A3
```

```
      SING=2.*A2*C1**(DLT/PI)*CDSQRT(EPS)/
     *       (CDSQRT(C2)*C3**(DLT/PI))
      DO 1 I=1,JMAX
        B=V(I)
        DB=B/100.
        BP=B+DB
        BM=B-DB
        A2P=A2+EPS
        RB=DREAL(B)
        RBP=DREAL(BP)
        RBM=DREAL(BM)
        P2=A2+2.*XI
        P3=RB+2.*XI
        P3P=RBP+2.*XI
        P3M=RBM+2.*XI
        CALL ROMBRG(1,A2P,P2,XINT)
        CALL ROMBRG(1,P2,P3,XINT1)
        CALL ROMBRG(1,P3,B,XINT2)
        CALL ROMBRG(1,P2,P3P,XINT1P)
        CALL ROMBRG(1,P3P,BP,XINT2P)
        CALL ROMBRG(1,P2,P3M,XINT1M)
        CALL ROMBRG(1,P3M,BM,XINT2M)
        ZM=XINT+XINT1M+XINT2M+SING
        Z(I)=XINT+XINT1+XINT2+SING
        ZP=XINT+XINT1P+XINT2P+SING
        DER(I)=((CDLOG((Z(I)-ZM)/(ZP-Z(I))))/(2.*DB))*
     *             (CDSQRT(B-A6)*CDSQRT(B-A2)*(B-A3)**(DLT/PI)/
     *              (B*(B-A5)**(DLT/PI)))
    1 CONTINUE
      RETURN
      END



      FUNCTION FUN2(X1,Z,DER)
      IMPLICIT INTEGER*4(I-N)
      COMPLEX*16 X1,Z,DER,XI,FUN2
      REAL*8     ERR,PI,ALP,APX,XK1,XK2,DLT,A2,A3,A5,A6
      COMMON /DATA2/ XI,ERR,PI
      COMMON /DATA3/ ALP,APX
      COMMON /DATA5/ XK1,XK2,DLT
      COMMON /DATA6/ A2,A3,A5,A6
      FUN2=APX*(2.*DCONJG(Z)+XI*(XK1+(1.-XK1)*CDEXP(-XI*DLT)))/
                                                  (XK1*ALP)
     *
     *    -(1.-1./((1./X1-1./DCONJG(X1))*(X1-DCONJG(X1))))
     *          *(CDSQRT(X1-A6)*CDSQRT(X1-A2)*(X1-A3)**(DLT/PI)/
     *           (X1*(X1-A5)**(DLT/PI)))
     *    -DER/(1./X1-1./DCONJG(X1))
      RETURN
      END
```

```
      SUBROUTINE VORTEX(W,GAM)
      IMPLICIT INTEGER*4(I-N)
      COMPLEX*16 W,XI
      REAL*8     ERR,PI,GAM,ALP,APX
      DIMENSION W(10),GAM(10)
      COMMON /DATA2/ XI,ERR,PI
      COMMON /DATA3/ ALP,APX
      GAM(1)=2.*PI*ALP/DREAL(XI*(1./W(1)-1./DCONJG(W(1))))
      WRITE(34,100)GAM(1)
100   FORMAT(/5X,'3. VORTEX STRENGTH'/
     *       8X,'VORTEX STRENGTH = ',D11.4/)
      RETURN
      END



      SUBROUTINE LIFT1(GAM,VW,CLW,CDW,CLF,CDF,CLT,CDT,CLL
     *                 ,TCL,TCD,RTOR,RTO)
      IMPLICIT INTEGER*4(I-N)
      COMPLEX*16 VW,X1,X2,X3,X4,ES,A2P,A3M,A3P,A6M,
     *           A5M,A5P,SING5,SING6,SING7,SING8,
     *           C1,C2,C3,C4,C5,C6,C7,C8,C9,ZZ,Z,
     *           XI,SING1,SING2,SING3,SING4,Z1,Z2,Z3,Z4,
     *           C10,C11,C12,C13,C14,C15,C16,X5,X6,Z5,Z6
      REAL*8     GAM,A2,A3,A5,A6,U,V,W,CP,ERR,PI,XK2,XK1,DLT,
     *           ALP,APX,CL1,CL2,CL3,CL4,CLW,CDW,CLF,CLT,CDT,
     *           CDF,CLL,RTOR,RTO,TCL,TCD,CL5,CL6
      DIMENSION VW(10),GAM(10),Z(700),CP(700)
      COMMON /DATA2/ XI,ERR,PI
      COMMON /DATA3/ ALP,APX
      COMMON /DATA5/ XK1,XK2,DLT
      COMMON /DATA6/ A2,A3,A5,A6
      ES=(A6-A2)/200.
      A2P=A2+ES
      A3M=A3-ES
      A3P=A3+ES
      A6M=A6-ES
      A5M=A5-ES
      A5P=A5+ES
      C1=A2-A5
      C2=A2-A6
      C3=A2-A3
      C4=A3-A5
      C5=A3-A6
      C6=A3-A2
      C7=A6-A5
      C8=A6-A2
      C9=A6-A3
      C10=-A6
      C11=-A2
      C12=-A5
```

```
      C13=-A3
      C14=A5-A6
      C15=A5-A2
      C16=A5-A3
      SING1=2.*A2*CDSQRT(ES)*C1**(DLT/PI)/
     *        (CDSQRT(C2)*C3**(DLT/PI))
      SING2=-PI*A3*C4**(DLT/PI)*(-ES)**((PI-DLT)/PI)/
     *        ((PI-DLT)*CDSQRT(C5)*CDSQRT(C6))
      SING3=PI*A3*C4**(DLT/PI)*ES**((PI-DLT)/PI)/
     *        ((PI-DLT)*CDSQRT(C5)*CDSQRT(C6))
      SING4=-2.*A6*C7**(DLT/PI)*CDSQRT(-ES)/
     *        (CDSQRT(C8)*C9**(DLT/PI))
      SING5=-C12**(DLT/PI)*(-ES)**2/
     *        (CDSQRT(C10)*CDSQRT(C11)*C13**(DLT/PI)*2)
      SING6=C12**(DLT/PI)*ES**2/
     *        (CDSQRT(C10)*CDSQRT(C11)*C13**(DLT/PI)*2)
      SING7=-A5*PI*(-ES)**((PI+DLT)/PI)/
     *    (CDSQRT(C14)*CDSQRT(C15)*C16**(DLT/PI)*(PI+DLT))
      SING8=A5*PI*ES**((PI+DLT)/PI)/
     *    (CDSQRT(C14)*CDSQRT(C15)*C16**(DLT/PI)*(PI+DLT))
      DO 10 I=1,101
        X1=A2P+(A3M-A2P)*FLOAT(I-1)/100.
        CALL ROMBRG(1,A2P,X1,Z1)
        Z(I)=Z1+SING1
        ZZ=Z(I)
        CALL VEL(VW,GAM,X1,ZZ,U,V,W)
10    CP(I)=1.+ALP**2-U**2-V**2-W**2
      DO 20 I=102,202
        X2=A3P+(-.357-A3P)*FLOAT(I-102)/100.
        CALL ROMBRG(1,A3P,X2,Z2)
        Z(I)=XI*XK1+SING3+Z2
        ZZ=Z(I)
        CALL VEL(VW,GAM,X2,ZZ,U,V,W)
20    CP(I)=1.+ALP**2-U**2-V**2-W**2
      DO 25 I=203,303
        X3=-.357+(-ES+.357)*FLOAT(I-203)/100.
        CALL ROMBRG(1,A3P,X3,Z3)
        Z(I)=XI*XK1+SING3+Z3
        ZZ=Z(I)
        CALL VEL(VW,GAM,X3,ZZ,U,V,W)

25    CP(I)=1.+ALP**2-U**2-V**2-W**2
      DO 30 I=304,404
        X4=ES+(.475-ES)*FLOAT(I-304)/100.
        CALL ROMBRG(1,ES,X4,Z4)
        Z(I)=XI*(XK1+(1.-XK1)*CDEXP(XI*DLT))+SING6+Z4
        ZZ=Z(I)
        CALL VEL(VW,GAM,X4,ZZ,U,V,W)
30    CP(I)=1.+ALP**2-U**2-V**2-W**2
      DO 40 I=405,505
        X5=.475+(A5M-.475)*FLOAT(I-405)/100.
        CALL ROMBRG(1,ES,X5,Z5)
```

```
        Z(I)=XI*(XK1+(1.-XK1)*CDEXP(XI*DLT))+SING6+Z5
        ZZ=Z(I)
        CALL VEL(VW,GAM,X5,ZZ,U,V,W)
40    CP(I)=1.+ALP**2-U**2-V**2-W**2
      DO 50 I=506,606
        X6=A5P+(A6M-A5P)*FLOAT(I-506)/100.
        CALL ROMBRG(1,A5P,X6,Z6)
        Z(I)=XI*XK1*SING8+Z6
        ZZ=Z(I)
        CALL VEL(VW,GAM,X6,ZZ,U,V,W)
50    CP(I)=1.+ALP**2-U**2-V**2-W**2
      CALL SIMP(Z,CP,CL1,CL2,CL3,CL4,CL5,CL6)
      CLW=(-CL6+CL1)
      CDW=CLW*ALP
      CLF=(-CL5+CL2)*DCOS(DLT)*(1.+ALP*APX*DTAN(DLT))
      CDF=(-CL5+CL2)*DCOS(DLT)*(ALP-APX*DTAN(DLT))
      CLT=(-CL4+CL3)*DCOS(DLT)*(1.+ALP*APX*DTAN(DLT))
      CDT=(-CL4+CL3)*DCOS(DLT)*(ALP-APX*DTAN(DLT))
      CLL=CLW+(-CL5+CL2-CL4+CL3)*DCOS(DLT)
      TCL=CLW+CLF+CLT
      TCD=CDW+CDF+CDT
      RTOR=1./ALP
      RTO=TCL/TCD
C     WRITE(34,100)
C     DO 46 I=1,406,5
C46    WRITE(34,200)Z(I),CP(I)
      WRITE(34,300)CLW,CDW,CLF,CDF,CLT,CDT,CLL,TCL,TCD,RTO,RTOR
100   FORMAT(20X,'Z',21X,'Cp',2X/)
200   FORMAT(10X,2D11.4,5X,D11.4)
300   FORMAT(//7X,'6.  LIFT BY INTEGRATION OF PRESSURE'//
     *          10X,'LIFT OF MAIN WING  = ',D11.4/
     *          10X,'DRAG OF MAIN WING  = ',D11.4/
     *          10X,'LIFT OF FLAP              = ',D11.4/
     *          10X,'DRAG OF FLAP              = ',D11.4/
     *          10X,'LIFT OF TAP        = ',D11.4/
     *          10X,'DRAG OF TAP        = ',D11.4/
     *          10X,' CHECK FOR LIFT    = ',D11.4/
     *          10X,'TOTAL LIFT        = ',D11.4/
     *          10X,'TOTAL DRAG         = ',D11.4/
     *          10X,'LIFT DRAG RATIO    = ',D11.4/
     *          10X,'IDEAL RATIO       = ',D11.4)
      RETURN
      END



      SUBROUTINE SIMP(Z,CP,CL1,CL2,CL3,CL4,CL5,CL6)
      IMPLICIT INTEGER*4(I-N)
      COMPLEX*16 Z
      REAL*8     CL1,CL2,CL3,CL4,CP,CL5,CL6
      DIMENSION Z(700),CP(700)
```

```
      CL1=0.
      CL2=0.
      CL3=0.
      CL4=0.
      CL5=0.
      CL6=0.
      DO 10 I=1,100
10    CL1=CL1+CDABS(Z(I+1)-Z(I))*(CP(I+1)+CP(I))/2.
      DO 20 I=102,201
20    CL2=CL2+CDABS(Z(I+1)-Z(I))*(CP(I+1)+CP(I))/2.
      DO 30 I=203,302
30    CL3=CL3+CDABS(Z(I+1)-Z(I))*(CP(I+1)+CP(I))/2.
      DO 40 I=304,403
40    CL4=CL4+CDABS(Z(I+1)-Z(I))*(CP(I+1)+CP(I))/2.
      DO 50 I=405,504
50    CL5=CL5+CDABS(Z(I+1)-Z(I))*(CP(I+1)+CP(I))/2.
      DO 60 I=506,605
60    CL6=CL6+CDABS(Z(I+1)-Z(I))*(CP(I+1)+CP(I))/2.
      RETURN
      END



      SUBROUTINE PRESSURE(VW,GAM)
      IMPLICIT INTEGER*4(I-N)
      COMPLEX*16 VW,X,ES,A2P,A3M,A3P,A6M,C1,C2,C3,C4,C5,C6,
     *           C7,C8,C9,XI,SING1,SING2,SING3,SING4,Z1,Z2,Z
      REAL*8     GAM,A2,A3,A5,A6,U,V,W,CP,ERR,PI,XK1,XK2,DLT
     *          ,ALP,APX
      DIMENSION VW(10),GAM(10)
      COMMON /DATA2/ XI,ERR,PI
      COMMON /DATA3/ ALP,APX
      COMMON /DATA5/ XK1,XK2,DLT
      COMMON /DATA6/ A2,A3,A5,A6
      WRITE(34,100)
      DO 200 I=1,41
        X=A2+(A6-A2)*FLOAT(I-1)/40.
        IF(DREAL(X).EQ.A2.OR.DREAL(X).EQ.A3.OR.
     *     DREAL(X).EQ.0..OR.DREAL(X).EQ.A5.OR.
     *     DREAL(X).EQ.A6) GO TO 200
        ES=(A6-A2)/200.
        A2P=A2+ES
        A3M=A3-ES
        A3P=A3+ES
        A6M=A6-ES
        C1=A2-A5
        C2=A2-A6
        C3=A2-A3
        C4=A3-A5
```

```
      C5=A2-A6
      C6=A3-A2
      C7=A6-A5
      C8=A6-A2
      C9=A6-A3
      SING1=2.*A2*CDSQRT(ES)*C1**(DLT/PI)/
     *      (CDSQRT(C2)*C3**(DLT/PI))
      SING2=-PI*A3*C4**(DLT/PI)*(-ES)**((PI-DLT)/PI)/
     *      ((PI-DLT)*CDSQRT(C5)*CDSQRT(C6))
      SING3=PI*A3*C4**(DLT/PI)*ES**((PI-DLT)/PI)/
     *      ((PI-DLT)*CDSQRT(C5)*CDSQRT(C6))
      SING4=-2.*A6*C7**(DLT/PI)*CDSQRT(-ES)/
     *      (CDSQRT(C8)*C9**(DLT/PI))
      IF(DREAL(X).LE.DREAL(A2P)) GO TO 200
      IF(DREAL(X).LT.DREAL(A3M)) GO TO 1
      IF(DREAL(X).LE.DREAL(A3P)) GO TO 200
      IF(DREAL(X).LT.DREAL(A6M)) GO TO 2
      GO TO 200
1     CALL ROMBRG(1,A2P,X,Z1)
      Z=Z1+SING1
      GO TO 300
2     CALL ROMBRG(1,A3P,X,Z2)
      Z=XI*XK1+SING3+Z2
300   CALL VEL(VW,GAM,X,Z,U,V,W)
      CP=1.+ALP**2-U**2-V**2-W**2
C     WRITE(6,*)Z,CP,U,V,W
      WRITE(34,400)Z,CP,U,V,W
200   CONTINUE
100   FORMAT(/5X,'4. PRESSURE DISTRIBUTION '/
     *      14X,'Z',18X,'Cp',11X,'U',12X,'V',12X,'W',1X)
400   FORMAT(4X,2D11.4,4(2X,D11.4))
      RETURN
      END



      SUBROUTINE VEL(VW,GAM,X,Z,U,V,W)
      IMPLICIT INTEGER*4(I-N)
      COMPLEX*16 VW,A,FUN4,X,Z,XI
      REAL*8     GAM,U,V,W,ERR,PI,ALP,APX,XK1,XK2,DLT
      DIMENSION VW(10),GAM(10)
      COMMON /DATA2/ XI,ERR,PI
      COMMON /DATA3/ ALP,APX
      COMMON /DATA5/ XK1,XK2,DLT
      A=FUN4(VW(1),GAM(1),X)
      V=DREAL(A)
      W=DREAL(XI*A)
      IF(DREAL(X).GT.0.) GO TO 1
      U=1.+DREAL(ALP*X+XI*GAM(1)*(CDLOG(X-VW(1))-
     *                  CDLOG(X-DCONJG(VW(1)))+2.*PI*XI)/(2.*PI)
     *          -DREAL(Z)*V-DIMAG(Z)*W)*APX/XK1
      GO TO 2
1     U=1.+DREAL(ALP*X+XI*GAM(1)*(CDLOG(X-VW(1))-
```

```
*                    CDLOG(X-DCONJG(VW(1))))/(2.*PI)
*           -DREAL(Z)*V-DIMAG(Z)*W)*APX/XK1
2     RETURN
      END



      FUNCTION FUN4(V,G,X)
      IMPLICIT INTEGER*4(I-N)
      COMPLEX*16 V,X,FUN4,XI
      REAL*8     G,ERR,PI,ALP,APX,XK1,XK2,DLT,A2,A3,A5,A6
      COMMON /DATA2/ XI,ERR,PI
      COMMON /DATA3/ ALP,APX
      COMMON /DATA5/ XK1,XK2,DLT
      COMMON /DATA6/ A2,A3,A5,A6
      FUN4=(ALP*XI*G*(1./(X-V)-1./(X-DCONJG(V)))/(2.*PI))
     *     *CDSQRT(X-A6)*CDSQRT(X-A2)*(X-A3)**(DLT/PI)/
     *      (X*(X-A5)**(DLT/PI))
      RETURN
      END



      SUBROUTINE LIFT(GAM,W,CL)
      IMPLICIT INTEGER*4(I-N)
      COMPLEX*16 W,XI,A2P,A3M,A6M,ES,C1,C2,C3,C4,C5,C6,C7,
     *           C8,C9,C10,XINT1,XINT2,XINT3,SING1,SING2,
     *           SING3,SING4,CLL
      REAL*8     GAM,CL1,CL2,CL,ALP,APX,XK1,XK2,DLT,A2,A3,A5,A6,
     *           ERR,PI
      DIMENSION GAM(10),W(10)
      COMMON /DATA2/ XI,ERR,PI
      COMMON /DATA3/ ALP,APX
      COMMON /DATA5/ XK1,XK2,DLT
      COMMON /DATA6/ A2,A3,A5,A6
      ES=(A6-A2)/100.
      C1=A2-A5
      C2=A2-A6
      C3=A2-A3
      C4=A3-A5
      C5=A3-A6
      C6=A3-A2
      C7=A6-A5
      C8=A6-A2
      C9=A6-A3
      C10=A5
      A2P=A2+ES
```

```
      A3M=A3-ES
      A6M=A6-ES
      CL1=2.*GAM(1)*DIMAG(W(1)-DCONJG(W(1)))*APX/
     *                    (XK1*(XK1+(1.-XK1)*DCOS(DLT)))
      CALL ROMBRG(2,A2P,A3M,XINT1)

      CALL ROMBRG(2,A3P,C10,XINT2)
      CALL ROMBRG(2,C10,A6M,XINT3)
      SING1=2.*A2**2*C1**(DLT/PI)*CDSQRT(ES)/
     *          (CDSQRT(C2)*C3**(DLT/PI))
      SING2=-PI*A3**2*C4**(DLT/PI)*(-ES)**((PI-DLT)/PI)/
     *          ((PI-DLT)*CDSQRT(C5)*CDSQRT(C6))
      SING3=-2.*A6**2*C7**(DLT/PI)*CDSQRT(-ES)/
     *          (CDSQRT(C8)*C9**(DLT/PI))
      SING4=PI*A3**2*C4**(DLT/PI)*ES**((PI-DLT)/PI)/
     *          ((PI-DLT)*CDSQRT(C5)*CDSQRT(C6))
      CLL=XINT1+SING1+SING2+XINT3+SING3
     *          +(XINT2+SING4)*DCOS(2.*DLT)
      CL2=-4.*ALP*DIMAG(CLL)*APX/(XK1*(XK1+(1.-XK1)*DCOS(DLT)))
      CL=CL1+CL2
      WRITE(6,*)CL1,CL2,CL
      WRITE(34,100)CL1,CL2,CL
100   FORMAT(/5X,'5. LIFT COEFFICIENTS. '/
     *        8X,' LIFT FROM VORTEX          = ',D11.4/
     *        8X,' LIFT FROM ATTACHED FLOW = ',D11.4/
     *        8X,' TOTAL LIFT                = ',D11.4/)
      RETURN
      END



      FUNCTION FUN5(X)
      IMPLICIT INTEGER*4(I-N)
      COMPLEX*16 FUN5,X,XI
      REAL*8     ERR,PI,XK1,XK2,DLT,A2,A3,A5,A6
      COMMON /DATA2/ XI,ERR,PI
      COMMON /DATA5/ XK1,XK2,DLT
      COMMON /DATA6/ A2,A3,A5,A6
      IF(DREAL(X).EQ.0..OR.DREAL(X).EQ.A5) GO TO 1
      FUN5=X**2*(X-A5)**(DLT/PI)/
     *     (CDSQRT(X-A6)*CDSQRT(X-A2)*(X-A3)**(DLT/PI))
      GO TO 2
1     FUN5=0.
2     RETURN
      END
```

```
      SUBROUTINE DECOMP(A,IPVT,OA)
      IMPLICIT INTEGER*4(I-N)
      IMPLICIT REAL*8(A-H,O-Z)
      DIMENSION A(10,10),WORK(10),OA(10,10),Z(10),IPVT(10)
      COMMON /DATA1/ IMAX,JMAX
      N=2*IMAX
      DO 1 I=1,N
        DO 1 J=1,N
        OA(I,J)=A(I,J)
1     CONTINUE
      IPVT(N)=1

      IF(N.EQ.1) GO TO 80
      NM1=N-1
      ANORM=0.
      DO 10 J=1,N
        T=0.
        DO 5 I=1,N
          T=T+DABS(A(I,J))
5       CONTINUE
        IF(T.GT.ANORM) ANORM=T
10    CONTINUE
      DO 35 K=1,NM1
        KP1=K+1
        M=K
        DO 15 I=KP1,N
          IF(DABS(A(I,K)).GT.DABS(A(M,K))) M=I
15      CONTINUE
        IPVT(K)=M
        IF(M.NE.K) IPVT(N)=-IPVT(N)
        T=A(M,K)
        A(M,K)=A(K,K)
        A(K,K)=T
        IF(T.EQ.0.) GO TO 35
        DO 20 I=KP1,N
          A(I,K)=-A(I,K)/T
20      CONTINUE
        DO 30 J=KP1,N
          T=A(M,J)
          A(M,J)=A(K,J)
          A(K,J)=T
          IF(T.EQ.0.) GO TO 30
          DO 25 I=KP1,N
            A(I,J)=A(I,J)+A(I,K)*T
25        CONTINUE
30      CONTINUE
35    CONTINUE
      DO 50 K=1,N
        T=0.
        IF(K.EQ.1) GO TO 45
        KM1=K-1
```

```
      DO 40 I=1,KM1
        T=T+A(I,K)*WORK(I)
40    CONTINUE
45    EK=1.
      IF(T.LT.0.) EK=-1.
      IF(A(K,K).EQ.0.) GO TO 90
      WORK(K)=-(EK+T)/A(K,K)
50  CONTINUE
    DO 60 KB=1,NM1
      K=N-KB
      T=0.
      KP1=K+1
      DO 55 I=KP1,N
        T=T+A(I,K)*WORK(K)
55    CONTINUE
      WORK(K)=T
      M=IPVT(K)
      IF(M.EQ.K) GO TO 60
      T=WORK(M)
      WORK(M)=WORK(K)
      WORK(K)=T
60  CONTINUE
    YNORM=0.
    DO 65 I=1,N
      YNORM=YNORM+DABS(WORK(I))
65  CONTINUE
    CALL SOLVE(A,WORK,IPVT,Z)
    ZNORM=0.
    DO 70 I=1,N
      ZNORM=ZNORM+DABS(Z(I))
70  CONTINUE
    COND=ANORM*ZNORM/YNORM
    IF(COND.LT.1.) COND=1.
    RETURN
80  COND=1.
    IF(A(1,1).NE.0.) RETURN
90  COND=1.E+32
    RETURN
    END
```

```
      SUBROUTINE SOLVE(A,B,IPVT,X)
      IMPLICIT INTEGER*4(I-N)
      IMPLICIT REAL*8(A-H,O-Z)
      DIMENSION IPVT(10),A(10,10),B(10),X(10)
      COMMON /DATA1/ IMAX,JMAX
      N=2*IMAX
      DO 1 I=1,N
        X(I)=B(I)
```

```
1       CONTINUE
        IF(N.EQ.1) GO TO 50
        NM1=N-1
        DO 20 K=1,NM1
          KP1=K+1
          M=IPVT(K)
          T=X(M)
          X(M)=X(K)
          X(K)=T
          DO 10 I=KP1,N
            X(I)=X(I)+A(I,K)*T
10        CONTINUE
20      CONTINUE
        DO 40 KB=1,NM1
          KM1=N-KB
          K=KM1+1
          X(K)=X(K)/A(K,K)
          T=-X(K)
          DO 30 I=1,KM1
            X(I)=X(I)+A(I,K)*T
30        CONTINUE
40      CONTINUE
50      X(1)=X(1)/A(1,1)
        RETURN
        END
```

End of Document